Jason Pryce Foster, 2LT, USAF
"An Examination of the Use of Geogrid as a Compaction Aid", 57 pages
Master of Science in Civil Engineering
Montana State University, 1999

ABSTRACT

Evidence from experimental and field applications suggest that the presence of geogrid in highway base course increases the ability of a granular material to compact. The addition of a geogrid into an aggregate base layer may decrease the lateral spreading of the base material as compaction effort is applied, leading to a greater potential for the base course to compact vertically.

The hypothesis being examined is that given an equal amount of compactive effort, geogrid reinforced base course material can achieve a greater density than non-reinforced base course. This hypothesis was evaluated by the construction of test sections with and without geogrid, compaction of these test sections using small field-scale equipment, and measurement of density and void ratio by various means. The effects of varying lift thicknesses and compactive efforts were also evaluated.

Changes in density were recorded with a nuclear densometer. A Dynamic Cone Penetrometer (DCP) was also used to indicate relative density of the base course. The third procedure for evaluating density and void ratio versus depth was accomplished via computer aided tomography (CAT). CAT combines ordinary X-ray technology with sophisticated computer signal processing and delivers digital images capable of being analyzed with selected software. The software was then used to calculate a series of void ratios for soil samples taken from the reinforced and non-reinforced sections. An average void ratio for each section was then computed and the results for each reinforced and non-reinforced section compared.

Based upon review of density results and DCP measurements, there does not seem to be a clear indication that geogrid reinforced base course material achieves a greater density than non-reinforced material given the same amount of compactive effort.

The void ratios obtained via CAT scan analysis do show a better distinction between the two configurations. Statistical analysis reveals that geogrid reinforced base course can achieve a higher density than non-reinforced base course at a confidence level of at least 96%.

REPORT DOCUMENTATION PAGE	Form Approved OMB No. 0704-0188

1. AGENCY USE ONLY *(Leave blank)*	2. REPORT DATE	3. REPORT TYPE AND DATES COVERED
	14.Feb.00	THESIS

4. TITLE AND SUBTITLE
AN EXAMINATION OF THE USE OF GEOGRID AS A COMPACTION AID

5. FUNDING NUMBERS

6. AUTHOR(S)
2D LT FOSTER JASON P

7. PERFORMING ORGANIZATION NAME(S) AND ADDRESS(ES)
MONTANA STATE UNIVERSITY

8. PERFORMING ORGANIZATION REPORT NUMBER

9. SPONSORING/MONITORING AGENCY NAME(S) AND ADDRESS(ES)
THE DEPARTMENT OF THE AIR FORCE
AFIT/CIA, BLDG 125
2950 P STREET
WPAFB OH 45433

10. SPONSORING/MONITORING AGENCY REPORT NUMBER
FY00-45

11. SUPPLEMENTARY NOTES

12a. DISTRIBUTION AVAILABILITY STATEMENT
Unlimited distribution
In Accordance With AFI 35-205/AFIT Sup 1

12b. DISTRIBUTION CODE

13. ABSTRACT *(Maximum 200 words)*

14. SUBJECT TERMS

15. NUMBER OF PAGES
52

16. PRICE CODE

17. SECURITY CLASSIFICATION OF REPORT	18. SECURITY CLASSIFICATION OF THIS PAGE	19. SECURITY CLASSIFICATION OF ABSTRACT	20. LIMITATION OF ABSTRACT

Jason Pryce Foster, 2LT, USAF
"An Examination of the Use of Geogrid as a Compaction Aid"

References

"Engineering Use of Geotextiles", Joint Departments of the Army and Air Force, TM 5-818-8/AFJMAN 32-1030, 20 July 1995.

Fannin, R. J. and Sigurdson, O. (1996) "Field Observations on Stabilization of Unpaved Roads With Geosynthetics", Journal of Geotechnical Engineering, Vol. 122, pp. 544-553.

Holtz, R. D. (1988) "Geosynthetics for Soil Improvement", Proceedings of the Symposium Sponsored by the Geotechnical Engineering Division of the American Society of Civil Engineers 1988, Special Publication No. 18, 211p.

John, N. W. M. (1997) "Geotextiles", Chapman and Hall: New York, 347p.

Kawamura, Toshiyuki. (1990) "Nondestructive, Three-Dimensional Density Measurements of Ice Core Samples by X-Ray Computed Tomography", Journal of Geophysical Research, August 10, 1990, Vol. 95, No. B8, pp. 12,407-12,412.

Koerner, R. M., and Soong, T. (1997) "The Evolution of Geosynthetics", Civil Engineering, Vol. 67, pp. 62-64.

Lynch, L. N., Webster, S. L., Bush III, A. J. (1996) "Expedient Surfaces", The Military Engineer, Aug/Sep 1996, pp. 32-33.

Moghaddas-Nejad, F. and Small, John C. (1996) "Effect of Geogrid Reinforcement in Model Track Tests on Pavements", Journal of Transportation Engineering, Vol. 122, pp. 468-74.

Perkins, S. W. (1999) "Geosynthetic Reinforced of Flexible Pavements: Laboratory Based Pavement Test Sections", Final Report for the State of Montana Department of Transportation, 17 March 1999.

Rao, P. V. (1998) "Statistical Research Methods in the Life Sciences", Duxbury Press: Boston.

Scudder, Henry J. "Introduction to Computer Aided Tomography", Proceedings of the IEEE, Vol. 66 No. 6, June 1978.

Van Santvoort, G. P. T. M. (1994) "Geotextiles and Geomembranes in Civil Engineering", A. A. Balkema: Rotterdam, Netherlands, 595p.

Van Santvoort, G. P. T. M. (1995) "Geosynthetics in Civil Engineering", A. A. Balkema: Rotterdam, Netherlands, 105p.

AN EXAMINATION OF THE USE OF GEOGRID AS A COMPACTION AID

by

Jason Pryce Foster

A professional paper submitted in partial
fulfillment of the requirements for the degree

of

Master of Science

in

Civil Engineering

MONTANA STATE UNIVERSITY-BOZEMAN
Bozeman, Montana

August 1999

APPROVAL

of a paper submitted by

Jason Pryce Foster

This paper has been read by each member of the paper committee and has been found to be satisfactory regarding content, English usage, format, citations, bibliographic style, and consistency, and is ready for submission to the College of Graduate Studies.

Steven W. Perkins _____ _____
(Signature) Date

Approved for the Department of Civil Engineering

Donald A. Rabern _____ _____
(Signature) Date

Approved for the College of Graduate Studies

Bruce R. McLeod _____ _____
(Signature) Date

Signature _____

Date _____

STATEMENT OF PERMISSION TO USE

In presenting this paper in partial fulfillment of the requirements for a master's degree at Montana State University-Bozeman, I agree that the Library shall make it available to borrowers under rules of the Library.

If I have indicated my intention to copyright this paper by including a copyright notice page, copying is allowed for scholarly purposes, consistent with "fair use" as prescribed in the U. S. Copyright Law. Requests for permission for extended quotation from or reproduction of this paper in whole or in parts may be granted only by the copyright holder.

Signature _____

Date _____

TABLE OF CONTENTS

LIST OF TABLES

LIST OF FIGURES

LIST OF CHARTS

LIST OF PHOTOGRAPHS

ABSTRACT

Evidence from experimental and field applications suggest that the presence of geogrid in highway base course increases the ability of a granular material to compact. The addition of a geogrid into an aggregate base layer may decrease the lateral spreading of the base material as compaction effort is applied, leading to a greater potential for the base course to compact vertically.

The hypothesis being examined is that given an equal amount of compactive effort, geogrid reinforced base course material can achieve a greater density than non-reinforced base course. This hypothesis was evaluated by the construction of test sections with and without geogrid, compaction of these test sections using small field-scale equipment, and measurement of density and void ratio by various means. The effects of varying lift thicknesses and compactive efforts were also evaluated.

Changes in density were recorded with a nuclear densometer. A Dynamic Cone Penetrometer (DCP) was also used to indicate relative density of the base course. The third procedure for evaluating density and void ratio versus depth was accomplished via computer aided tomography (CAT). CAT combines ordinary X-ray technology with sophisticated computer signal processing and delivers digital images capable of being analyzed with selected software. The software was then used to calculate a series of void ratios for soil samples taken from the reinforced and non-reinforced sections. An average void ratio for each section was then computed and the results for each reinforced and non-reinforced section compared.

Based upon review of density results and DCP measurements, there does not seem to be a clear indication that geogrid reinforced base course material achieves a greater density than non-reinforced material given the same amount of compactive effort.

The void ratios obtained via CAT scan analysis do show a better distinction between the two configurations. Statistical analysis reveals that geogrid reinforced base course can achieve a higher density than non-reinforced base course at a confidence level of at least 96%.

CHAPTER 1: INTRODUCTION

The field of geosynthetics includes geotextiles, geomembranes, geogrids, geonets, geocomposites, and all other similar materials used by civil engineers to improve or modify the behavior of soil (Holtz, 1988). Civil engineering and construction disciplines have seen a gradual increase in the use and application of geosynthetic materials from development in the Netherlands in the 1950s (Van Santvoort, 1994). Since their rise to popularity in the mid-1960s, however, geosynthetic materials have maintained a steady rate of growth as their construction applications broaden. Usage of geosynthetics has matured to the point where these products can no longer be considered as "new" materials. Today, dynamic economic and environmental factors have made the geosynthetic industry over a billion dollar per year market (Koerner and Soong, 1997). Continued research and development investigates ways in which geosynthetics can provide longer lasting and less expensive job performance than current designs (Koerner and Soong, 1997). Ongoing use and expansion of geosynthetics is proving to make both engineering logic and economic sense.

Functions of Geosynthetic Materials

Geosynthetic materials act as reinforcement to soils used in foundations, highways, side slopes, and in other geotechnical engineering functions as liquid drainage and leakproof barrier systems (Van Santvoort, 1994). Pertinent to this paper are compaction applications, which occur frequently in highway-related applications. Multiple studies have evaluated the benefits of using geosynthetic materials as

reinforcement in the base course and subgrade of highways. While engineering designs utilizing geosynthetics continue to be refined, some of the economic benefits deserve more intense study. Documentation has proven that geosynthetics can increase the load bearing capacity, lifespan, and durability of highways. It is also known that geosynthetics can span areas of problem soils to enable suitable road construction. Economic benefits are seen in the smaller amounts of engineering base course material required due to the added strength geosynthetics build into the design.

The engineering benefits of geogrids specifically come from two primary functions, reinforcement and lateral restraint. The reinforcement helps to distribute concentrated loads over larger areas of the subgrade to avoid overloading of the subgrades' bearing capacity. Figure 1 below shows a geosynthetic reinforcing the base course to reduce the load on the subgrade.

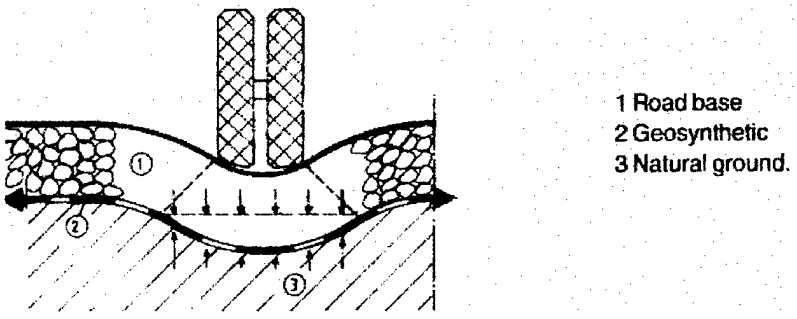

Figure 1. Reinforcement of Road Base Course with Geosynthetic (Van Santvoort, 1995)

In construction over soils with very low bearing capacities, the geogrid helps to redistribute loads to reduce soil pressures.

The purpose of the reinforcement function is to add tensile properties to soil, much in the same way that reinforcing steel is used with concrete. In both cases, materials with good compressive properties (soil and concrete) are combined with

materials with good tensile properties (geogrids, geotextiles, and steel) to construct a structure with adequate compressive and tensile strengths.

Lateral restraint reduces the amount of horizontal deformation seen in the base course and the subgrade where they are in contact with the geogrid (Van Santvoort, 1994). Figure 2 is a simplified version of the cross-section of a typical highway base course layer used as a specific example. Initially the material is loosely consolidated; if a vertical compressive load is applied to this layer, the material will consolidate vertically while spreading laterally. Maximum vertical compaction cannot occur because of the fact that there is lower resistance to the vertical stress as the material is able to relieve the stress by spreading laterally.

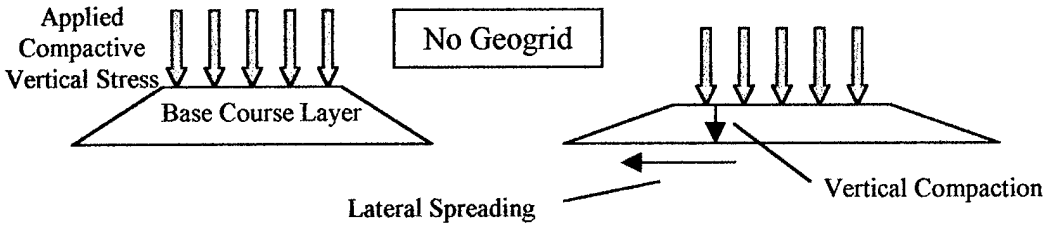

Figure 2. Vertical Compaction and Lateral Spreading of an Unreinforced Base Course Cross-Section

It is reasonable to assume, therefore, that reduction of lateral spreading may increase the amount of vertical compaction in the base course when compactive effort is applied. The use of a geogrid is one such way in which lateral spreading can be reduced. Figure 3 illustrates this point. The geogrid causes particle interlock with the lower levels of base course. These particles lock with the particles above, which in turn lock with particles above, and so on. Because material cannot spread laterally as easily as before, greater compaction may be achieved vertically.

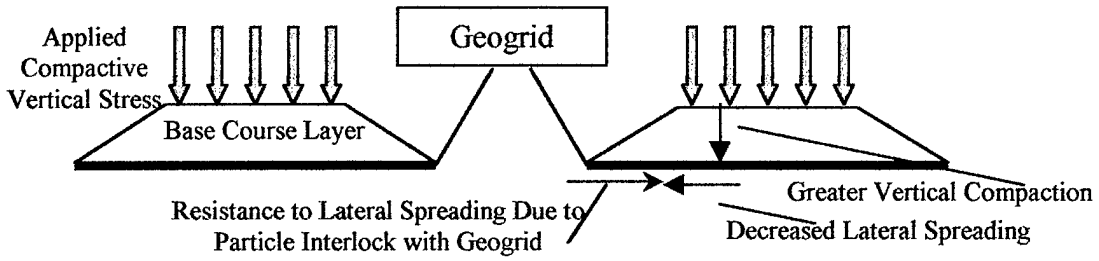

Figure 3. Vertical Compaction and Lateral Spreading of a Geogrid Reinforced Base Course Cross-Section

Design and Manufacture of Geogrids

The structure and manufacture of geogrids is integral to the design and application of these materials. Geogrids are "polymer planar structures consisting of a regular open network of integrally connected tensile elements" (Van Santvoort, 1994). In other words, geogrids are a plastic netting with adequate thickness to provide resistance to tension forces in soil loading applications. There are two primary ways in which geogrids are manufactured that impact the tensile characteristics of the material.

The first manufacturing process begins with an extruded sheet of polyethylene or polypropylene that is then punched with a regular pattern of holes. The form, size, and distribution of the holes are pre-determined by the end characteristics desired in the geogrid. Under the application of direct heat, the sheet is then stretched into an ordered and aligned state. This stretching process increases the tensile strength and stiffness of the polymer and creates the open structure needed to allow particle interlock (Van Santvoort, 1994). A uniaxial geogrid offers tensile resistance in one direction only. A biaxial geogrid provides tensile resistance in two planar directions.

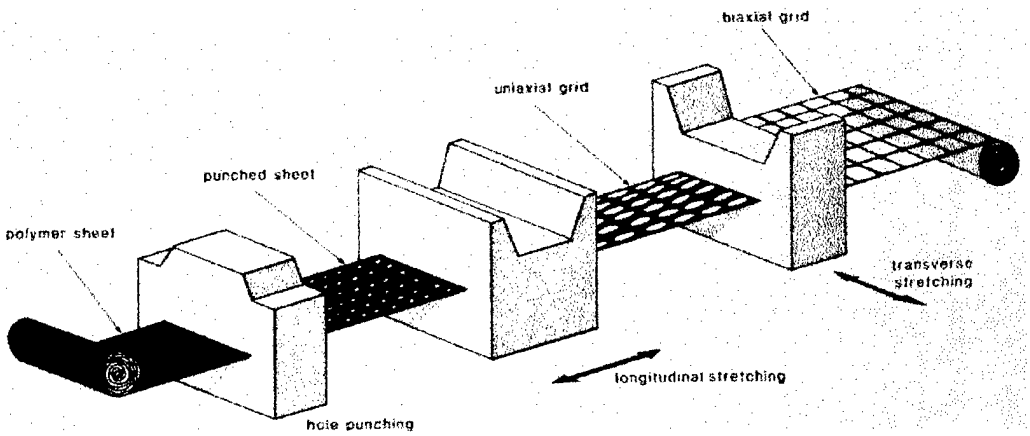

Figure 4. Manufacturing Sequence for Biaxial Geogrids (John, 1987)

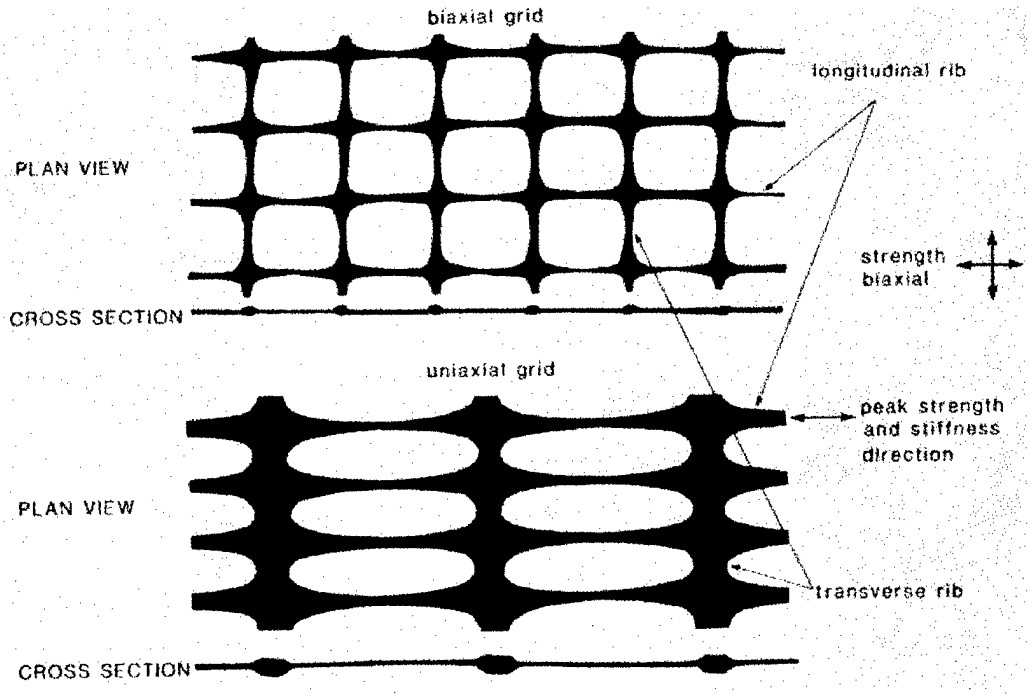

Figure 5. Uniaxial and Biaxial Geogrids (John, 1987)

The second process hinges on the concept of the welded strip grid. This type consists of two sets of geotextile strips that intersect at 90 degrees and are heat welded at the intersections (John, 1987).

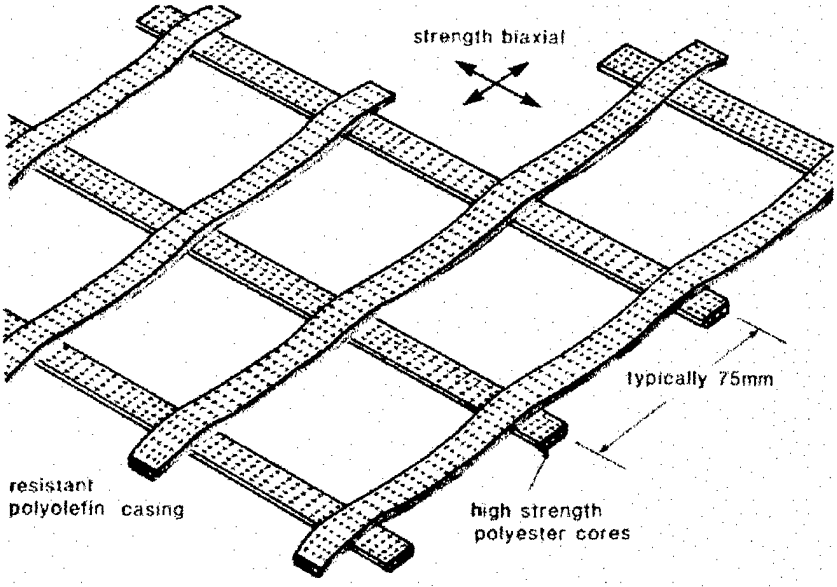

Figure 6. Welded Strip Geogrid (John, 1987)

Advantages of Geogrid Utilization

Geogrids offer many advantages in the design and construction of longer-lasting, lower-maintenance roadways, runways, parking lots, and other paved surfaces. In addition, geogrids offer speed and economize construction over weak soils and can improve the overall performance of the entire flexible pavement system regardless of the underlying soil conditions. When used with select base course material, the geogrid-reinforced construction platform can eliminate the need to undercut existing soils, and the usage of imported fill or chemical stabilizers. Geosynthetics enable road construction in what were once trouble areas and reduce the costs spent on road building materials.

A highway design that cuts back on equipment and labor has the potential for greater highway design efficiency. As highway funding continues to dwindle, increased attention has shifted to the productivity and efficiency of new engineering projects. One of the primary and most vital aspects of highway construction is compaction of the base course aggregate. Numerous compactor passes are needed to ensure that road base

materials are compacted to the design levels fulfilling requirements of the highway system. The reduction of compaction costs, therefore, promises to have overriding benefits for highway construction.

Military Engineering Applications for Geogrids

The pace of military deployment around the world demands continued efforts to improve the flexibility and expediency of engineering forces to support the mission crucial assets in any theater of operations. In addition, the stationing of construction equipment and personnel in remote and underdeveloped locations with minimal pavement infrastructure continues to be problematic. The United States Armed Forces are continually looking to the civilian section and their own research organizations to deliver techniques and materials that expedite construction time while reducing building and maintenance costs that drives these efforts.

While the military is currently evaluating the various benefits that geosynthetic materials offer in world-wide deployment, the current design standard for use of geotextiles is very limited. Current as of 20 July 1995, the Air Force Joint Manual (AFJMAN) 32-1030 contains little design consideration for geotextiles and absolutely no design aids incorporating geogrids (Army and Air Force, 1995). As more research is conducted, refined, and applied, the military will eventually see that the construction of roads and airfields utilizing geogrids will meet the requirements of cost efficiency, mission capability, and expedient and flexible methodologies in design and construction. The deployable abilities of United States' military forces could be greatly enhanced with the addition of geogrids to airfield design in underdeveloped locations.

Previous Geogrid Research and Documentation

Previous research for most geogrid performance testing in geogrid reinforced highways use rut depth as the comparing engineering characteristic to evaluate geosynthetically reinforced and non-reinforced roadways. In an oval test track setup, Moghaddas and Small (1996) discovered that for a thin base layer, the amount of rutting could be drastically lowered with the inclusion of a geogrid. It was found that the least amount of surface deformation was obtained with the geogrid at the center of the base layer. Tests utilizing the geogrid at the interface between the base course and subgrade showed that there were still significant advantages to geogrid reinforcement in other locations (Moghaddas and Small, 1996). Moghaddas and Small go on to suggest that the main mechanism for reinforcement is interlocking of the granular material and confinement of the base layer. The effect of the grid prevents lateral expansion of the base material. Fannin and Sigurdson (1996) also found that the use of a geogrid significantly improved the performance of unpaved roads. Their testing was done in the field in a continuous course alternating between unreinforced and reinforced section utilizing both geogrids and geotextiles (Fannin and Sigurdson, 1996).

Testing has shown that geogrids can increase the load bearing capacity and lifespan of highways. In addition, evidence suggests that geogrids may allow an increased density to be achieved with a specific level of compactive effort (compared to non-reinforced soils). This evidence therefore suggests that geogrid reinforcement may allow for a decrease in the amount of compactive effort needed to compact base course layers. The geogrid laterally restrains the base course in place; greater compaction then occurs in the vertical direction. Base course material without the benefit of geogrid may

actually have translation in the horizontal direction that lessens the amount of compaction that can be seen vertically.

This theory leads to the hypothesis examined by this work. The addition of a geogrid into an aggregate base layer may decrease the lateral spreading of the base material as compaction effort is applied. This is accomplished via the interlocking mechanism the aggregate particles achieve with the open net structure of the geogrid. Now that the lateral movement of the base material is somewhat restricted, greater vertical stresses are achieved and lead to greater compaction.

The Waterways Experiment Station (WES), the research arm of the Army Corps of Engineers, has conducted various research with geosynthetic materials that are most pertinent to this paper. Both field and laboratory evaluations using punched sheet drawn polypropylene geogrids show that base course thicknesses could be reduced by up to 50% by placing the grid between the base aggregate and subgrade soil. This testing has also shown that the geogrid actually increases the compaction of the gravel base course, giving the base layer more strength (Lynch et. al., 1996). This evidence helps to form the basis behind this particular investigation.

Therefore, if geogrids can increase the amount of vertical compaction in base course and overall density of the soil layer, then the base course can achieve accepted density levels with fewer compactor passes compared to non-reinforced soil. The economic implications of this hypothesis suggest that additional evaluation is needed. Testing may show that the cost and time required for base course preparation might be decreased if geogrids do indeed have the anticipated effect.

Project Origin

Tensar Earth Technologies, Incorporated, approached Montana State University to explore the research hypothesis described earlier. Evidence from experimental and field applications suggested that the presence of the geogrid increased the ability of a granular base course material to compact. No direct research of this hypothesis has been performed prior to this work.

The Department of Civil Engineering at Montana State University possesses a specific piece of equipment that was useful in pursuing this work. A Digital Radiography—Computed Tomography (DR/CT) scanner system, more commonly known as a CAT (computed axial tomography or computer-aided tomography) scanner can readily measure the void space and orientation of soil and rock particles. While other universities would physically "slice" soil core samples and count the amount of void space, the DR/CT system and associated software could more easily deliver consistent, economical, and repeatable results. Tensar desired to have more extensive data than nuclear densometer readings to analyze the change in density between reinforced and non-reinforced soil profiles.

Paper Overview

The remainder of this paper will address the details of the project proposal and execution. It will discuss the various methods and equipment used to fully examine the testable hypothesis. The results analysis portion of the hypothesis is based upon Computed Aided Tomography (CAT), a relatively new technology with very little history in the evaluation of soil characteristics. This paper will examine the theory behind this

emerging tool and the various methods undertaken to arrive at a suitable procedure for its implementation.

In addition, this paper will address the field testing facility and the necessary steps taken to evaluate the hypothesis. From project proposal to project execution, and CAT feasibility investigations to calibration and analysis, this paper will outline the steps of this research unique to the geotechnical engineering world.

CHAPTER 2: HYPOTHESIS AND TESTING

Introduction to Hypothesis and Testing Methodology

Experimental Hypothesis

The hypothesis being examined in this paper is that given an equal amount of compactive effort, geogrid reinforced base course material can achieve a greater density than non-reinforced base course. This hypothesis was evaluated by the construction of test sections with and without geogrid, compaction of these test sections using small field-scale equipment, and measurement of density and void ratio by various means.

If the above hypothesis proves to be true, it is based on the belief that decreased lateral spreading of the base material occurs due to the addition of a geogrid into the aggregate base layer. This decrease in lateral spreading is accomplished via the interlocking mechanism the aggregate particles achieve with the open net structure of the geogrid. Because the lateral movement of the base material is restricted, greater vertical stresses are achieved leading to greater vertical compaction. Therefore, based on the same amount of compactive effort, geogrid reinforced base course aggregate is capable of greater density that non-reinforced base course aggregate.

Should hypothesis validation result from the testing, the effect on the engineering profession would be primarily economic. Use of geogrid in highway applications may result in the need for fewer compactor passes. If the design reduces the amount of compaction needed to achieve a specified density, the savings on equipment and labor would be substantial. Labor and equipment costs constitute the majority of highway

construction costs. Therefore, a sizeable reduction in these costs leads to great overall savings in the project.

Besides the possible monetary savings resulting from geogrid use, another benefit may be the expediency geogrid use brings to the design of other geotechnical engineering designs requiring specialized compaction specifications. Highways and airfields are two the most obvious applications that may have tremendous utility from the use of geogrid. This could have a great impact on the military, especially when it comes to design and construction in rapid deployment exercises and engagements. The sooner a road is constructed, the sooner the troops and supply lines can bolster the allies. The quicker an airfield is built, the quicker the aircraft can deliver the needed assets to sustain forces and gain an advantage against the enemy. Time is money in the civilian sector; time is a matter of life and death in the military.

Overview of Hypothesis Testing

This project was designed to adequately model field compaction procedures in the attempt to test the hypothesis. However, the testing needed to be designed so as to limit the variation in materials, compactive effort, and testing and analysis methods. The inclusion of geogrid in the design was to be the only variable; all other aspects of the project were to remain as consistent as possible.

Testing Apparatus

The model chosen to duplicate field procedures consisted of a two-foot high plywood box with plan dimensions of seven-feet by ten-feet. The soil inside the box consisted of twelve inches of weak clay subgrade overlain by twelve inches of a well-

graded gravel base course. One half of the box had the geogrid at the interface of these two materials.

The materials within the box were prepared to achieve uniformity of water content and density prior to any compaction. The compactor then traveled down the centerline of the test box only and delivered uniform compactive effort to the reinforced and non-reinforced sections. Final testing of the soil in the field apparatus was followed by excavation and retrieval of soil specimens.

Parameter Measurement for Hypothesis Testing

A variety of methods were used to determine the density of the base course material in order to compare the reinforced and non-reinforced sections. Void ratio is another parameter related to density that was used to evaluate the effect of geogrid on compaction of base course material.

Density

The actual density measurements of the base course were taken with a nuclear densometer prior to and after compaction. This self-contained unit returned timely results and showed how the density changed before and after compaction given the presence or absence geogrid. One of the main limitations of the nuclear densometer is the way in which it presented results. Rather than being able to show a decrease in density with depth at a specific location, the nuclear densometer reports the average density over a particular soil depth (typically six inches). While quick and easy to use, the nuclear densometer leaves room for more detailed investigation of the density of reinforced and non-reinforced samples.

California Bearing Ratio

Another representative measure of density is the Dynamic Cone Penetrometer (DCP). This method provided the advantage over the nuclear densometer of being able to provide an indication of density versus depth. The DCP values were correlated to California Bearing Ratio (CBR) values. Though CBR values are primarily used to evaluate the support strength of subgrade, the DCP results helped to provide as much extra information as possible to adequately evaluate the hypothesis. The DCP results provided additional information to help fill in the density versus depth gap left by the nuclear densometer.

Void Ratio

The third and most meticulous procedure for evaluating density and void ratio versus depth was accomplished via computer aided tomography (CAT). Computer aided tomography was used to analyze the void ratio in the reinforced and non-reinforced samples over a range of depths.

Montana State University-Department of Civil Engineering possesses such a machine capable of measuring the void ratio versus depth. The $380,000 Digital Radiography – Computed Tomography (DR/CT) scanner was produced by Synergistic Detector Designs of Sunnyvale, California. Scion Image software utilized the scanned images to determine void ratio. The detailed theory of this technique will be discussed in more detail later in the paper.

Mr. Mike Edens, the chief operator of the device, has worked exclusively with the scanner since August of 1997 and with Scion Image software since 1995, analyzing specimens from ice to asphalt. An exhaustive literature review revealed that little or no

work has been performed utilizing a DR/CT to measure void ratio in soil samples, also aligned with the limited reference Mr. Edens has seen on the subject. This project entered new geotechnical engineering territory by evaluating void ratio from a new and promising technique. The DR/CT scanner is shown in Photograph 1 below.

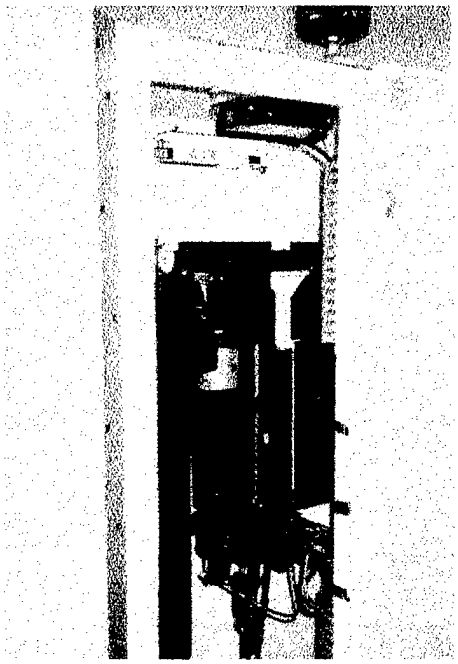

Photograph 1. MSU's DR/CT Scanner

The physical size of the DR/CT scanner did place limitations on the size of the soil specimen that could be analyzed. The soil samples needed to be no taller than twelve inches or bigger than four inches in diameter. These size limitations then placed restrictions on the potential excavation methods to be used in the test box described earlier. Also, the specimens needed to remain intact and undisturbed so as to provide an accurate representation of the reinforced and non-reinforced sections.

Hypothesis Testing Methodology

Test Box Design

The hypothesis testing apparatus utilized a wooden test box holding a one-foot layer of clay overlain by one foot of an aggregate base course material. The box was made of 5/8-inch plywood and had inside dimensions measuring ten feet by seven feet. The long sides were 24 inches high with the shorter end sides being 12 inches tall. 2x4 studs spaced horizontally and vertically along all sides provided structural reinforcement of the box. Photograph 2 shows the box with some uncompacted clay.

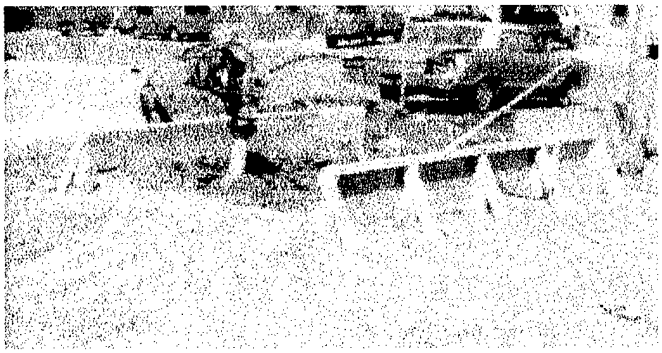

Photograph 2. Test Box with Uncompacted Clay

The soil profile consisted of 12 inches of a clay subgrade overlain by 12 inches of gravel base course. One half of the box used Tensar BX 1200 geogrid at the interface between the two soils; the other half had no reinforcement.

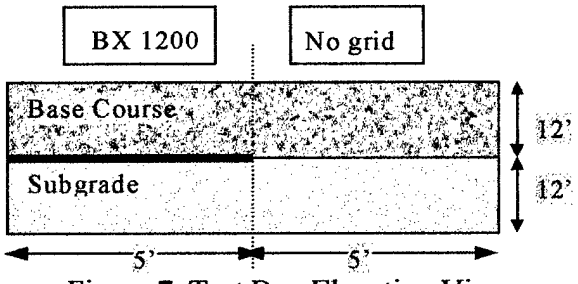

Figure 7. Test Box Elevation View

This entire experiment hinged on the ability to keep all parameters the same; the presence of the geogrid should be the only variable. Compactive effort applied to the base course was made as consistent and equal as possible with a Wacker RD880 3500-pound vibratory compactor. It was run down the center of the box and back along the centerline. The width of the compactor drum was 36 inches. Figure 8 shows the two-foot gap between the ends of the drum and the sides of the box.

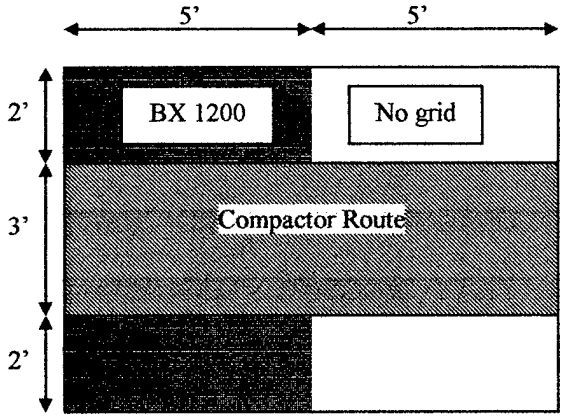

Figure 8. Test Box Plan View

Materials Used

Subgrade

A highly plastic clay (CH) was used as the test section subgrade. This material had a liquid limit of 100% and a plastic limit of 40%. All of the particles contained in this clay pass the #200 sieve (Perkins, 1999). During the course of the experiment the target water content was 43%, resulting in the target CBR value of 1.5. However, a water content of anywhere from 39% to 47% would return a CBR value between 3.0 and 1.5 to model a weak subgrade.

Base Course

The base course material classified as a well-graded gravel (GW). As shown by the following grain size distribution chart, 30% of the material was retained on the 10.0-millimeter sieve and 30% of the material passed the 2.0-millimeter sieve. The desired water content was 5%. The selection of this number is based upon requirements for sample retrieval. Prior to CAT scanning the soil samples were frozen. It was shown that in samples with water contents higher than 5%, the ice bonding was too difficult to overcome and the samples were unworkable. The selected water content yielded workable and durable specimens.

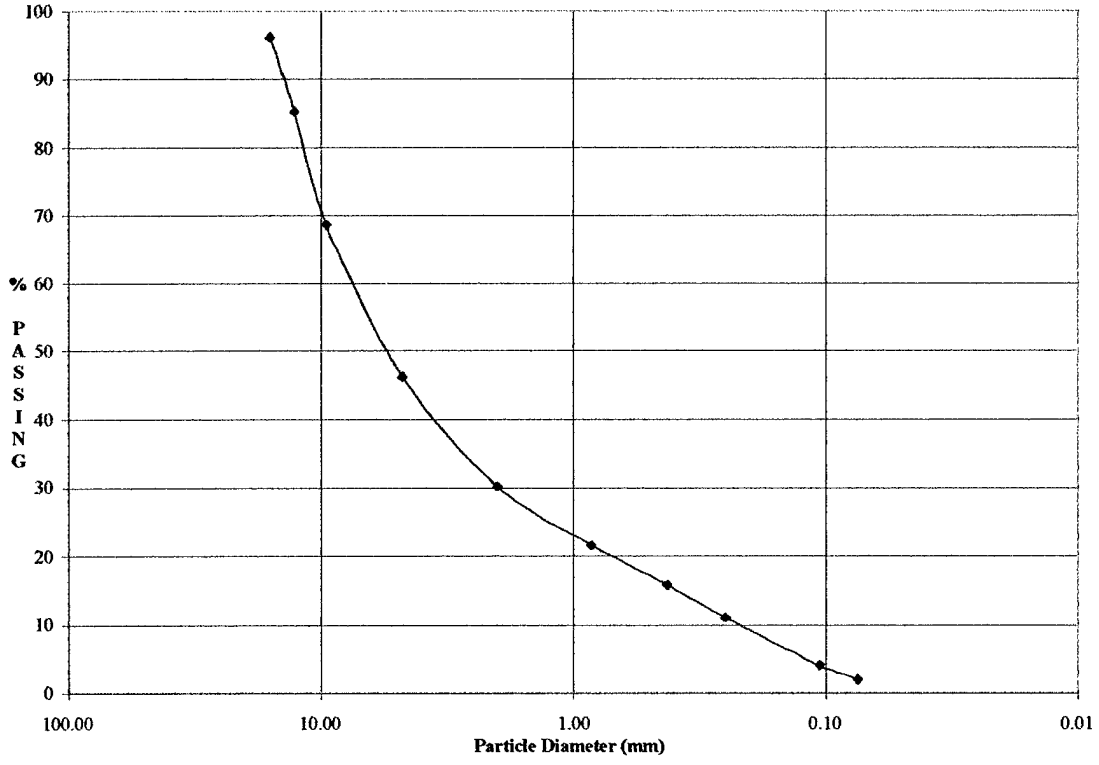

Chart 1. Grain Size Distribution Curve for Base Course Material

Composition of Phases/Sections

The testing utilized two other variables in the evaluation of the hypothesis: lift thickness of the base course and number of compactor passes. Table 1 shows the actual parameters for each of the test sections.

	Lift Thickness	Number of Compactor Passes
Section #1	12 inches	4
Section #2	12 inches	12
Section #3	2 – 6 inch lifts	4
Section #4	2 – 6 inch lifts	12

Table 1. Test Section Configurations

Test Section Procedure

A series of construction, testing, and excavation steps make up the testing procedure. This following figure represents a basic sequence for each test section.

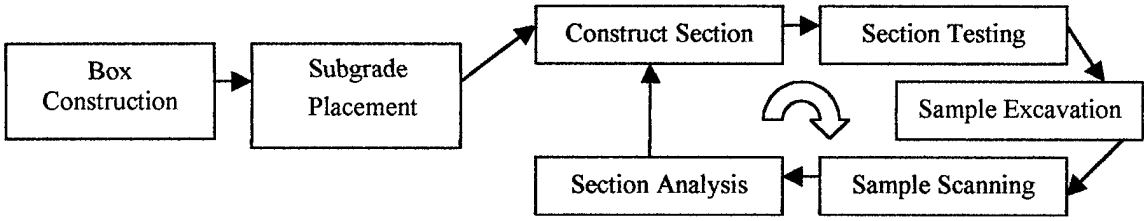

Figure 9. Test Section Procedure

Box Construction and Subgrade Placement

When the test box was first constructed at its outdoor testing location, plastic was laid to prevent drying of the clay subgrade. The subgrade was placed in the box one time.

Prior to the placement of base course in each test section, rod and level measurements helped to create as level of a subgrade surface as possible. Density and

water contents were also taken, and the DCP used to arrive at an approximate CBR value. The DCP readings were then taken for the first five blows only, which generally penetrated the entire subgrade.

Figure 10 shows the locations in which the various tests were conducted.

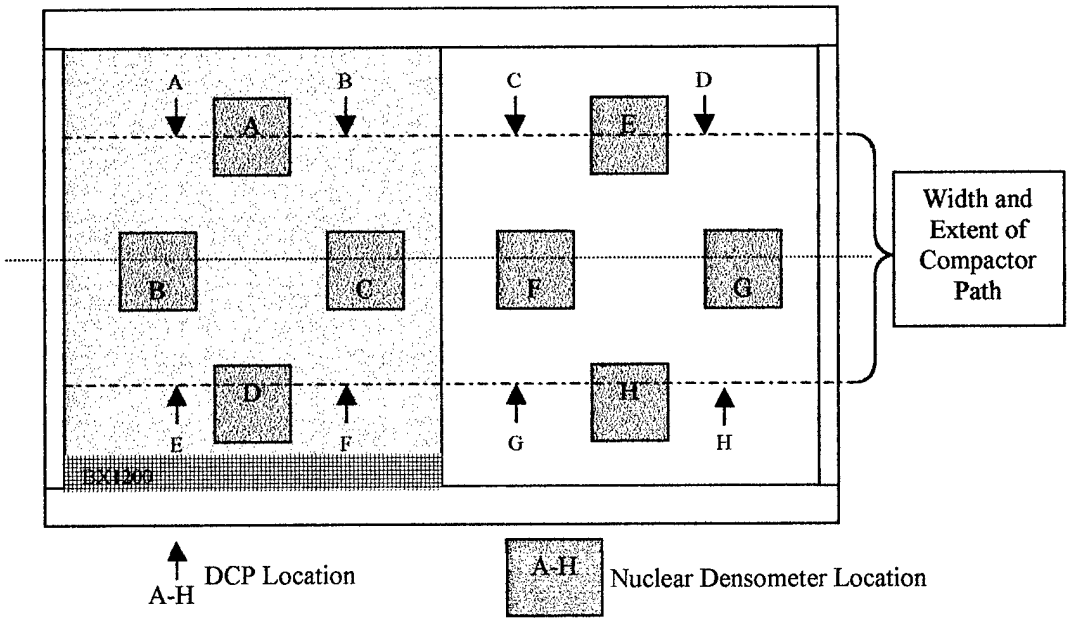

Figure 10. Subgrade Testing Locations

Photograph 3 shows the subgrade with rod and level measurements being taken. Also shown is the jumping jack compactor used to compact the subgrade.

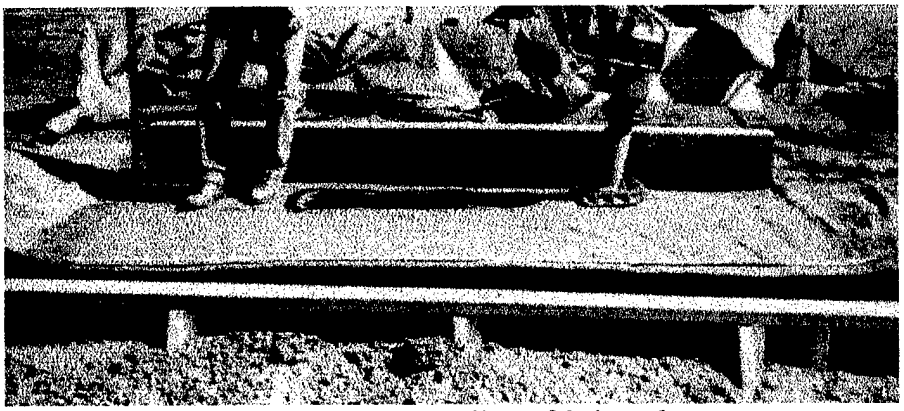

Photograph 3. Leveling of Subgrade

The table below summarizes the average CBR values of the subgrade obtained for each test section. These values are based upon readings for five blows into the subgrade. Both the reinforced and non-reinforced sections have four locations in which the reading were taken. Therefore, a total of twenty blow measurements compute each average CBR value.

	Grid			No-Grid		
	CBR	Water Content, %	Dry Density, pcf	CBR	Water Content, %	Dry Density, pcf
Test Section #1	2.7	39.8	71.8	2.2	39.1	73.4
Test Section #2	2.3	37.4	74.7	2.4	37.0	75.6
Test Section #3	2.8	40.4	69.2	2.6	39.6	70.1
Test Section #4	3.1	42.4	69.1	3.1	40.2	73.4

Table 2. Subgrade CBR, Water Contents, and Dry Density Values for Test Sections 1-4

Section Construction

A Bobcat loader was used to mix the base course material to the desired water content of five percent. Some of the base course material was placed in a thin layer over the subgrade in order to properly seat the geogrid for each test section. Photograph 4 shows the grid in place over half of the test box.

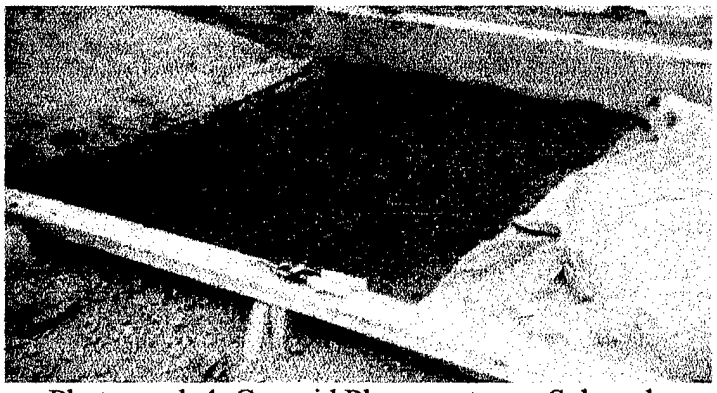

Photograph 4. Geogrid Placement over Subgrade

Once the base course water content was adequate, it was dumped into the test box. Shovels and rakes were used to spread the gravel around the box to the predetermined elevation. Care was taken to ensure that no personnel stepped on the uncompacted base course and caused compaction. Caution during the dumping and spreading made the initial dry densities as uniform as possible between the reinforced and non-reinforced halves. Photograph 5 shows the base course being dumped and raked.

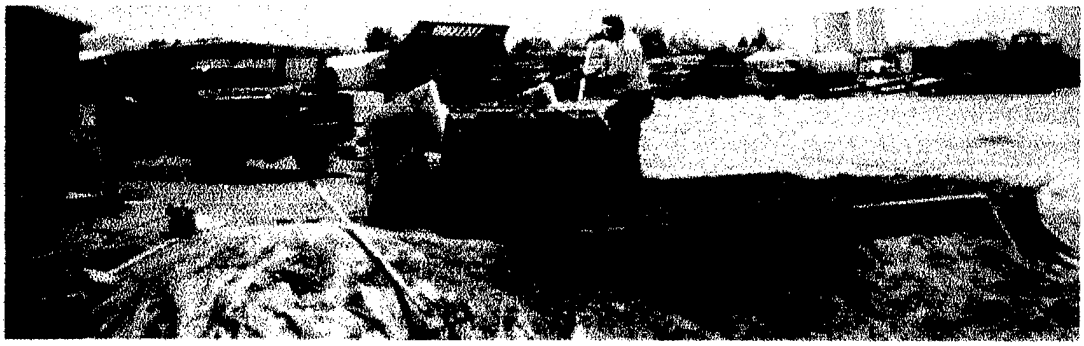

Photograph 5. Dumping and Spreading of Base Course

Pre-compaction measurements of density and elevation were taken at various locations in the box. The elevation readings ensured that the base course was as level and consistent as rake grooming could allow. Figure 11 shows the location in which the base course was tested.

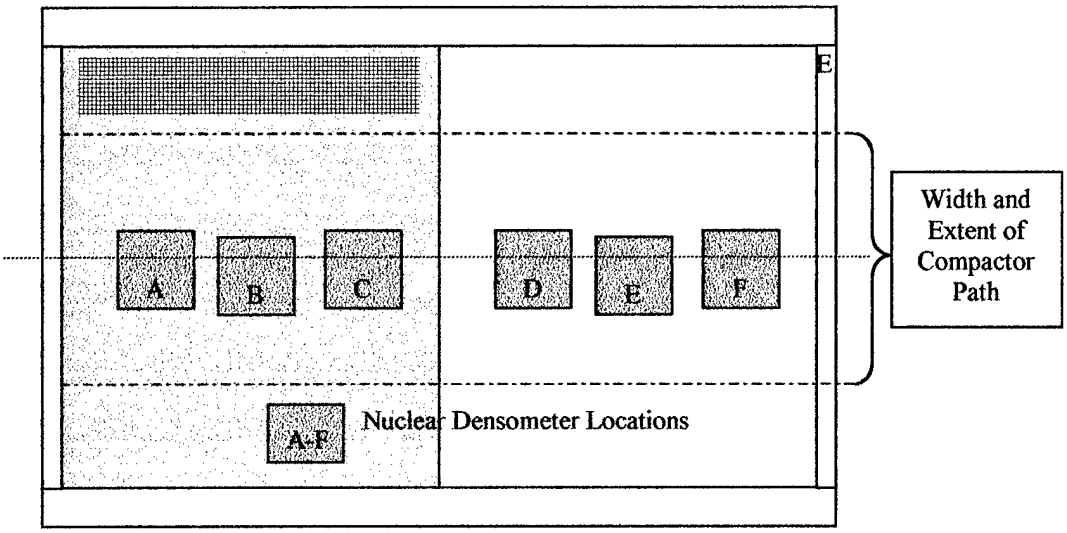

Figure 11. Base Course Pre-Compaction Testing Locations

When the pre-compaction measurements were finally obtained, the Wacker RD880 compactor was rolled into place. The number of passes were dependent upon the pre-determined characteristics of the particular test section. While one individual rode the compactor, another spotted the driver down the centerline and the other spotted over the ends.

Photograph 6. Compacting the Base Course

After compaction the follow-up measurements of density and elevation were performed. If the lift was the final lift for the test section, DCP testing was also performed. In addition, the location of the core samples was also marked. Figure 12

shows the locations of post-compaction measurements and where the soil samples were to be excavated.

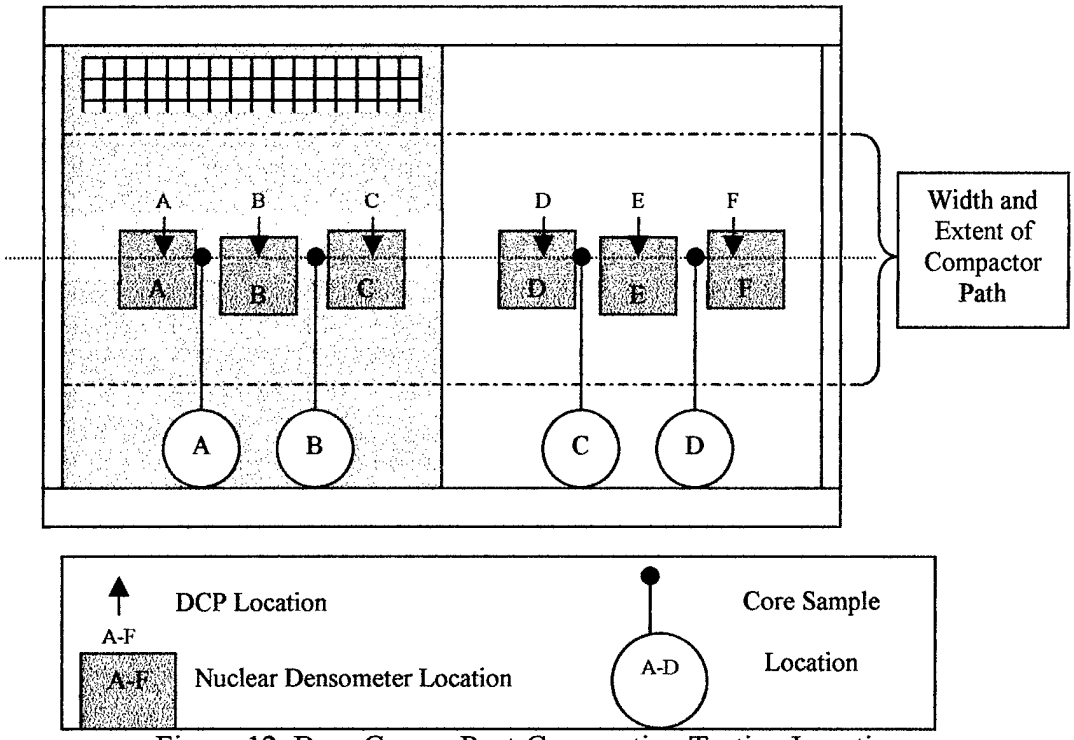

Figure 12. Base Course Post-Compaction Testing Locations

Whereas DCP readings were taken for the first five blows in the subgrade, the base course DCP displacements were recorded up and until enough blows pushed the DCP well into the subgrade. Photograph 7 shows the nuclear densometer and rod and level measurements being taken. Photograph 8 shows the DCP testing.

Photograph 7. Base Course Post-Compaction Nuclear Densometer and Rod and Level Measurements

Photograph 8: DCP Test on Compacted Base Course with Box Excavation Locations

Section Excavation

It was vital that soil samples used in the CAT scanner be as undisturbed as possible. The test box facility was located approximately three miles from the university. Therefore, reasonable "bulk" samples were first taken at the test site, transported in the back of a pickup truck back to the university, and later trimmed into the required scanning size.

Twelve-inch cubic wooden boxes were constructed to alleviate the problem associated with hauling the soil samples to the CAT scanning office. These particle board boxes had four sides with no bottom. The idea was to excavate base course material, slide a wooden box over the soil cube, then backfill the wood box with gravel so as to add "packing material" to the bulk soil sample. Then, in order to separate the base course from the clay, a metal clay undercutter was constructed. This apparatus was simply a piece of thin sheet metal reinforced by angled steel. The undercutter sliced through the clay and then acted as a bottom to the four-sided wooden transportation box. These soil cubes were transported and frozen prior to the working down to a 4-inch

diameter size. The following photograph shows the excavated base course, a wooden transportation box, and the clay undercutter prior to undercutting the subgrade.

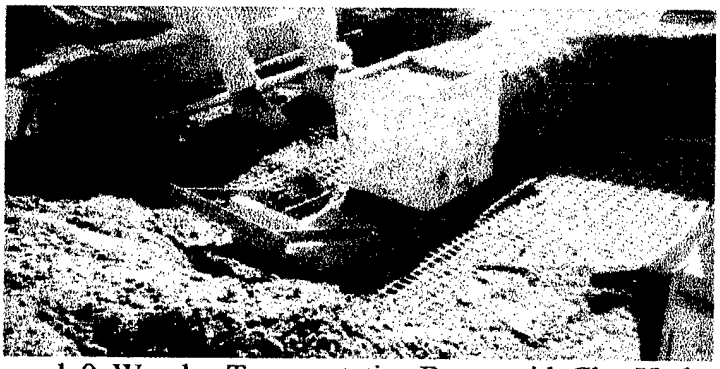

Photograph 9. Wooden Transportation Boxes with Clay Undercutter

Sample locations were kept consistent across all sections and marked with paint prior to any removal of gravel. Shovels, picks, rakes, and gloved hands were then used to remove the gravel out of the test box. Once the wooden boxes could encase the soil cubes, the clay was undercut. Project employees leg-pressed the apparatus through the entire layer, allowing the sheet metal to slice through the clay. The entire sample was then removed and prepared for travel back to University.

Photograph 10. Undercutting the Clay

Once the soil cubes were adequately frozen, the specimens could be trimmed to the 4-inch diameter cores. The sides of the transport boxes were first stripped off and any loose material brushed away. Because of the very rigid nature of the frozen soil cube, both hammer and chisel were used with the aid of a heat gun. As the coring process progressed, the diameter of the sample was routinely checked in order to make sure that a 4-inch cylinder could encase the sample. Though the following photograph lacks clarity, one can make out the core samples between their cube and 4-inch diameter state.

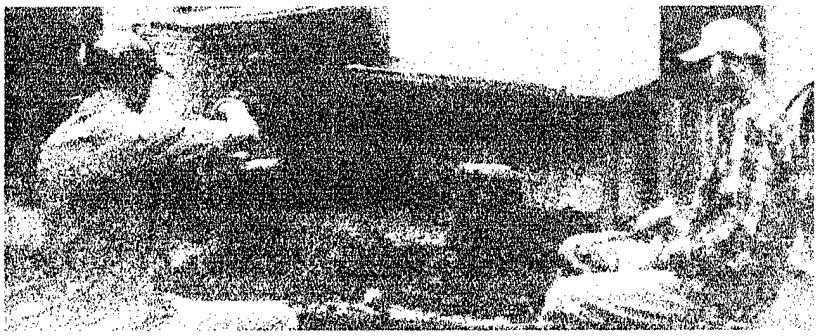

Photograph 11. Obtaining the Soil Columns from Frozen Soil Cubes

Once the proper soil heights and diameters were achieved, the test cylinders were sealed with saran wrap and duct tape to prevent moisture loss. In addition, the section number, test location, top or bottom sample, and direction to surface were indicated to make sure there would be no confusion during the scanning analysis.

Sample Scanning

The cross-sectional images as obtained from the DR/CT scanner are at first in grayscale, similar to that of a black and white photograph. There are varying levels of black, white, and gray contrast. Figure 13 shows a typical image taken from one of the test section core samples. Notice how the sample exterior does not touch the barely visible concrete test cylinder. This is due to the excavation complications.

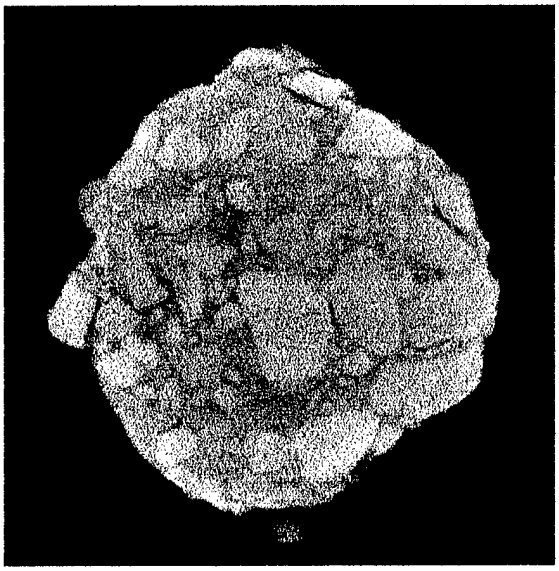

Figure 13. Typical Scanned Image

However, in order to count the void spaces, the image must be turned into a binary image made of only black or white. A computer program written for this project converts the grayscale image into a binary image. A copy of this program is shown in Appendix A.

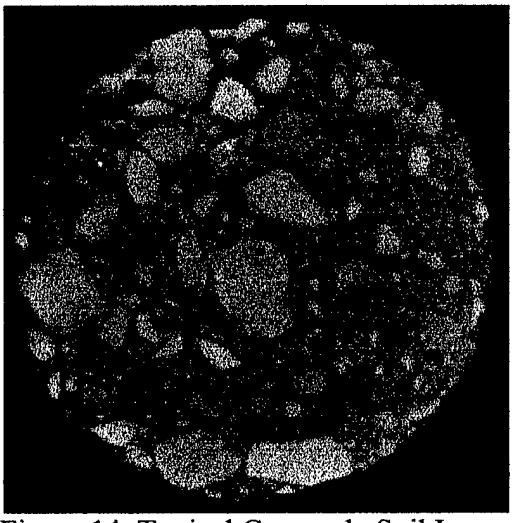

Figure 14. Typical Grayscale Soil Image

Figure 14 shows one an image from one of the calibration cylinders. Notice once again how the image contains varying levels of black and white contrast. Built into the

computer program for the image analysis is a parameter called the "standard deviation threshold." This command essentially works like a digital diode. A threshold is preset; if the input value is high enough, the computer reads that specific pixel as a 1 or a white pixel (or a soil particle). If the input intensity does not meet this specific threshold, then the computer counts that pixel as a 0 or a black pixel (in this case a void space). Therefore, the software looks at the intensity of grayscale at each pixel, determines if it meets the predetermined threshold value, and then assigns a black or white pixel based upon the value to threshold comparison. Figure 14 shows the scanned grayscale soil image while Figure 15 shows the binary image of this scan with the standard deviation threshold applied.

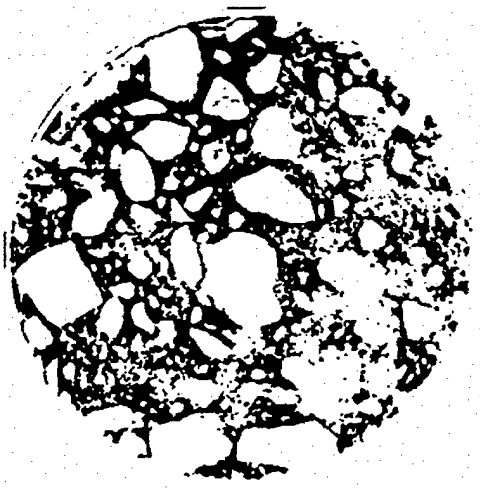

Figure 15. Typical Soil Image with Standard Deviation Threshold Applied

The computer operator now selected an interior portion of the binary cross-section to analyze for void ratio calculation. Figure 16 shows a typical selected area and the "Results" box that displays the resulting image void ratio.

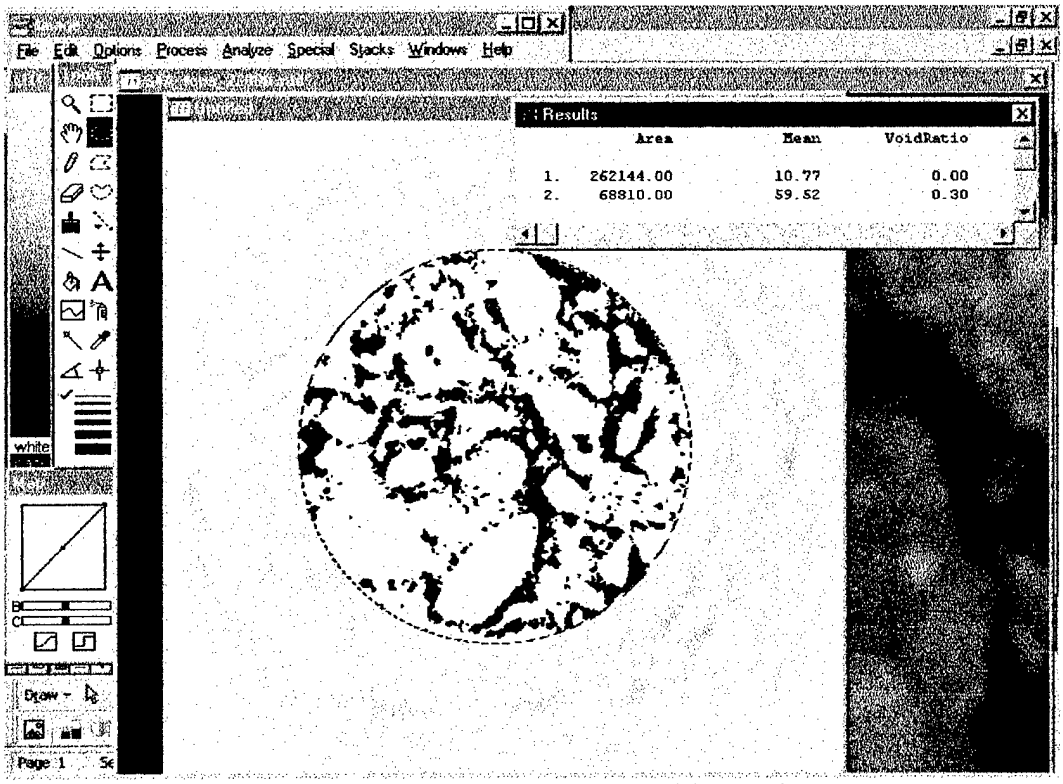

Figure 16. Analyzed Soil Area with Results

Four core samples were taken from each test section, two with reinforcement and two without. The scanning was performed in one-centimeter increments. Therefore, each core sample had approximately 28 scans over the twelve-inch depth. The resulting void ratios and depths were input into a spreadsheet and graphed.

All of the measured parameters had now been obtained. Changes in density were recorded, the DCP measurements correlated, and the void ratio data for each test section evaluated. The next test section commenced construction, starting with the subgrade leveling and testing.

Computer-Aided Tomography

Despite the fact that little to no research incorporating soil analysis and computer-aided tomography was found, the application of CAT to other materials has been used for

two decades. Therefore, extensive calibration of the scanning method and accompanying image analysis was needed for soil specimens. The most efficient and reliable scanning and analysis methods were developed and continually refined until a suitable procedure was produced.

Before getting into the details of how this procedure was developed, the theory of CAT will be discussed. The next section will show that despite the limited soil analysis based on CAT, evidence does exist that computer-aided tomography is suitable for this particular application.

The Scientific Theory of Computer Aided Tomography

The medical profession has used X-ray machines for years to detect broken bones, tumors, and other body ailments. The continued development of this technology has spread to various other applications with impressive results.

Computer-Aided Tomography (CAT) combines ordinary X-ray technology with sophisticated computer signal processing. A sending unit first emits the X-rays. Different materials then attenuate X-rays differently. The X-ray detection mechanism is electrical, with the resulting image a result of the accumulated attenuation of the original beam. The electronic data is then converted from an analog signal to digital impulses. The digital representation of the X-ray intensity is fed into a computer, which then reconstructs an image (Scudder, 1978).

An ordinary X-ray machine covers a plane in a single view, with height and width in the resulting picture. CAT limits the thickness or height of the X-ray beam to very small increments (usually much less than 1 centimeter) and scans in a single line of view. In addition, rotation of either the specimen or the X-ray projector obtains a three hundred

sixty-degree view of the object. While a typical X-ray is a two-dimensional representation of a three-dimensional object, a CAT scan is a two dimensional image of a single plane or cross section within a three-dimensional object. The result is a much clearer representation for a particular plane of interest (Scudder, 1978).

DR/CT Scanner Engineering Applications

Digital Radiography/Computed Tomography (DR/CT), an alternate name for the field of computer-aided tomography, is relatively new to the medical profession and is still expanding to new engineering applications. One of the primary uses of this technology has been in the study of deep ice cores in Greenland and Antarctica to obtain years of climatic records trapped within the ice. The bulk density of bubbly ice cores is widely used as one of the basic physical properties of these particular specimens. A study by Kawamura showed that the DR/CT scanner is a "potentially promising tool for nondestructive measurement of three-dimensional distribution of density and air bubbles" in the ice core samples from glaciers and ice sheets (Kawamura, 1990). There had been no attempt to apply this technique to the investigations of ice core density; similarly, there has been no recorded attempt to apply the DR/CT technology to the analysis of soil samples.

CAT is one of the promising nondestructive methods to calculate density and void ratio in soil samples. CAT allows the investigator to obtain the physical properties of the specimen and a window to the internal makeup of the sample. In Kawamura's work density results of the DR/CT scanner were calibrated to traditional density measurements for these particular ice samples. In the same light, the same techniques were applied to the uncharted territory of soil analysis with CAT techniques.

Initial CAT Scanning Feasibility and Calibration

Preliminary tests conducted in January and February of 1999 documented the capabilities of the DR/CT system. These tests focused primarily on methods for soil sample retrieval, scanning and measurement of void space, and calibration of software and procedures to accepted void ratio determination.

The first few calibration samples consisted of base course aggregate compacted into concrete test cylinders. These cylinders possessed a known volume. In addition, the soil and water weights were also recorded. Previous testing of the base course aggregate also assigned a specific gravity to the material. Therefore, the necessary parameters were available to calculate the void ratio in the cylinder based upon the traditional relationships between weight, volume, and specific gravity.

Once it had been proven that the average void ratio obtained from software analysis could match reasonably well with traditional calculations, the method of sample retrieval was developed. Additional testing showed that this base material could be compacted into a 12-inch wooden box, frozen, and then chipped into to 4-inch diameter by 12-inch high soil columns. Concrete test cylinders were used to encase these samples.

Just as the void ratio could be calculated for material compacted into a concrete test cylinder, the average void ratio present in the 12-inch box could also be determined. Some of the soil samples obtained from this sample retrieval investigation were also scanned. The void ratio from the resulting image analysis was compared with the preliminary calculated void ratio. Once again the traditional and scanned void ratios compared reasonably well.

Scanning Method Evaluation

The next step in the development of an acceptable CAT image analysis procedure involved the frequency and spacing of scans. While a large number of scans would give the best estimate of void ratio, they would also require much time and computer memory space.

Two distinct methods were evaluated that obtained images throughout the core samples. The first method, Method 1, used six thin scans around a central location, with each scan approximately .1 mm thick. Each of the cross-section images was then separately analyzed. Method 2 consisted of one image that was a pure average of the six images obtained in Method 1.

The greater the amount of data points, the more likely the sample mean is closer to the real mean. However, the greater the number of data points, the longer it takes for analysis. The great utility of Method 2 was the relative speed in which results could be obtained. Method 2 was proven to estimate Method 1 with adjustment of the standard deviation threshold in the image analysis methodology. Chart 2 shows the void ratios obtained at the various points for Method 1 with a standard deviation threshold of .35 and Method 2 with standard deviation thresholds of .35 and .45. Notice how the data points in Method 2 were moved to fit within the data scatter range of Method 1.

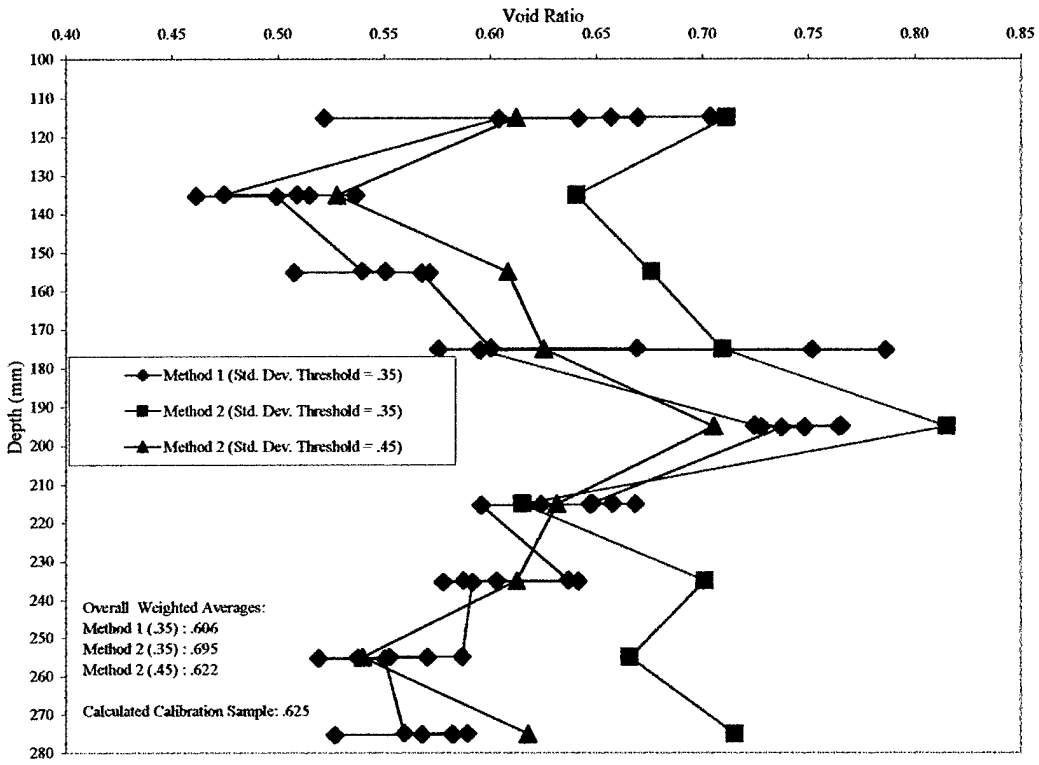

Chart 2. Comparison of Method 1 and Method 2

Because it had proven that Method 2 could accurately reflect Method 1, Method 2 was the chosen scanning method utilized in the following image analysis procedure discussion.

Digital to Binary Image Methodology Development

Three additional calibration cylinders were prepared for fine-tuning of the image analysis process. Calibration samples #3 and #4 were compacted in 4 lifts over the 8-inch height; calibration sample #5 was compacted in one 8-inch lift.

The initial analysis procedure using Scion Image was altered many times over the course of the calibration phase. The first method, Method A, used two copies of the same grayscale image for analysis. The first step required the selection of the soil area within

the confines of the concrete test cylinder. Next, all of the information outside of the selected region was removed. This resulting grayscale image with the removed outside area was then copied and transformed so that the entire area within the selected area was turned into black. This image was used to get the total area with the selected region. The original image then had the standard deviation threshold applied so that the grayscale became black and white, a true binary image. Finally, various counting procedures determined the number of black and white pixels in the original image and the number of black pixels in the copied image. These numbers were then put into a spreadsheet that determined the actual void ratio for the particular image.

Once all of the void ratios for each of the images at the specific locations had been determined, the overall average sample void ratio was calculated. While Method A did prove that it could deliver consistent results, a more simplified method was desired. The procedures associated with Method A required a tremendous amount of time.

Familiarization with Method A allowed for better understanding of the steps needed to properly analyze the images. The monotonous routine and time consumption pushed the desire to derive a more efficient methodology. The resulting Method B used the same pull-down menu steps of Method A. However, rather than using one black image to calculate total area and another image to determine percent black and white, the new pixel counting procedure used only one image. The separate black image was not required to calculate the total area present in the sample. This procedure could automatically determine the number of white and black pixels in the image. Method B increased the rate at which images could be processed.

The standard deviation thresholds had to then be adjusted so that the image analysis results followed the calculated void ratios. The chart below shows how a new standard deviation threshold value was determined for Method B.

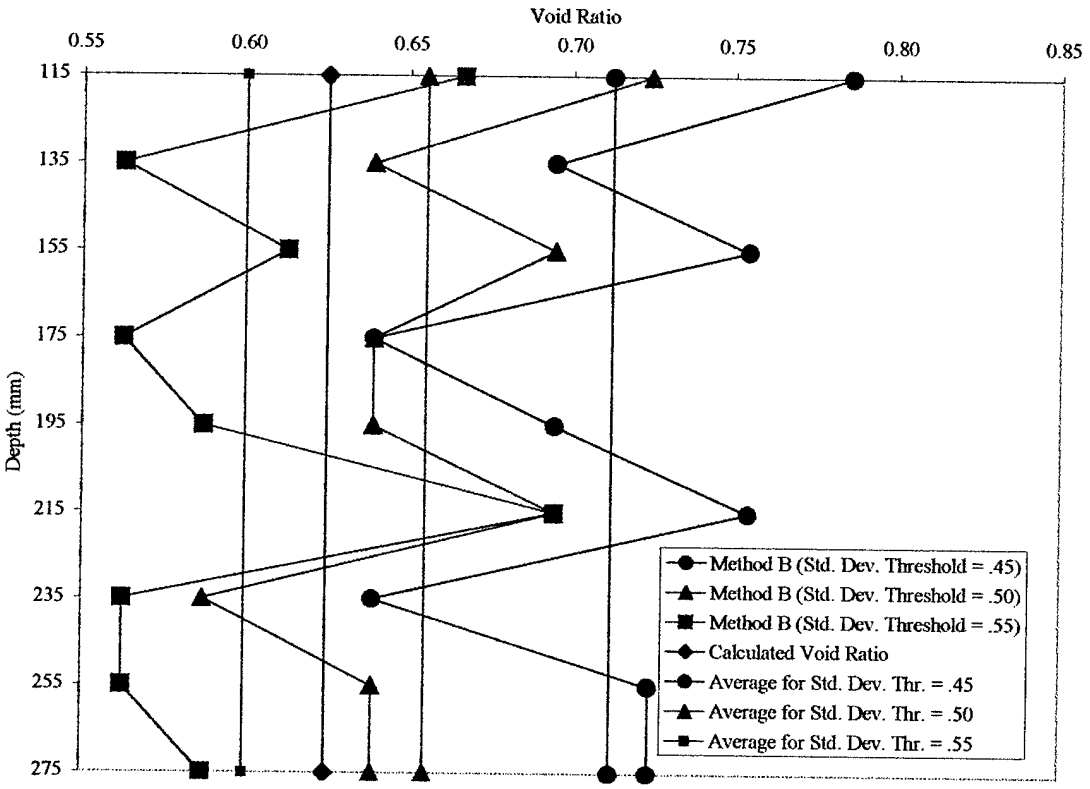

Chart 3. Calibration Sample #3: Method B Void Ratio Results for Various Standard Deviation Thresholds

Method B at a standard deviation threshold value of .45 produced void ratios higher than the pre-calculated value. Therefore, values of .5 and .55 were used to determine the average void ratio at these other levels. As the chart shows above, the calculated void ratio fell in between the average void ratios obtained from the .5 and .55 standard deviation threshold values. The new deviation threshold value was set to .525 so as to make Method B follow the calibrated void ratio.

Method B differed from Method A in that only one image was used and a simplified, more automated, pixel counting procedure utilized. Also, the standard

deviation threshold value applied to the images was re-calibrated. Method B proved to be a more expedient method of image analysis.

Even though the image analysis process had been made faster with the change to Method B and the standard deviation threshold altered to provide consistent results, a tremendous amount of tedious work was still required. In order to increase efficiency and reduce analysis errors even more, the image analysis process was written into a macro computer program. Much like a Pascal computer program, this macro used written text to direct the computer through commands that were once accomplished via pull down menus. This "Method X" became the final method used to analyze the scanned images for the test sections. The increase in rate of analysis was increased 300% with the formulation of the "Soil Analysis" computer program. The actual macro program is shown as Appendix A.

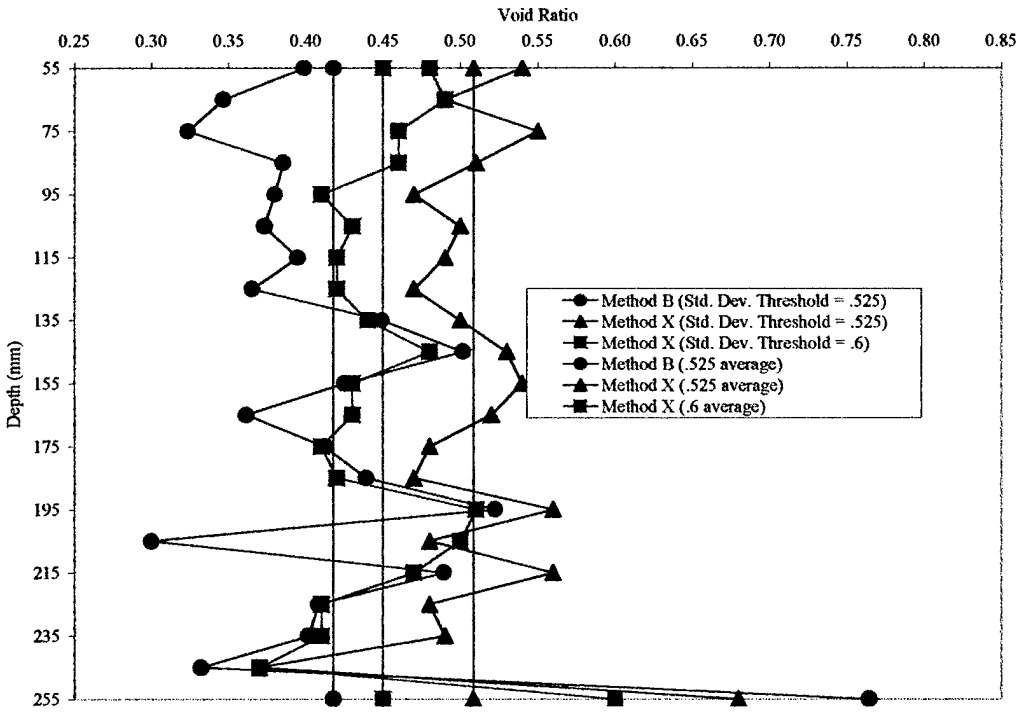

Chart 4. Calibration Sample #4: Method B versus Method X

The chart above shows the first attempt in evaluating Method B against Method X. Notice that the standard deviation threshold used in Method B (.525) needed to be increased in Method X so that a better correlation could be observed.

Even though the procedures of Method X were almost exactly the same as Method B, some error is introduced with each image analysis because the computer operator selects the area to analyze. Therefore, each time and area is selected and analyzed in Method X, the area is slightly different from that selected in Method B. This accounts for some of the error and variation between the two methods. Additional reasons for the discrepancies are not understood at this time.

Because of the fact that Method X could analyze images much quicker than Method B, more investigations were conducted to see if a different standard deviation threshold could deliver more accurate results for all three of the calibration cylinders.

The first iterations utilized the original standard deviation threshold value of .525. After evaluating multiple other values, a new value of .6 was written into the computer program. The following charts show how the average void ratios compared for both .525 and .6 standard deviation thresholds.

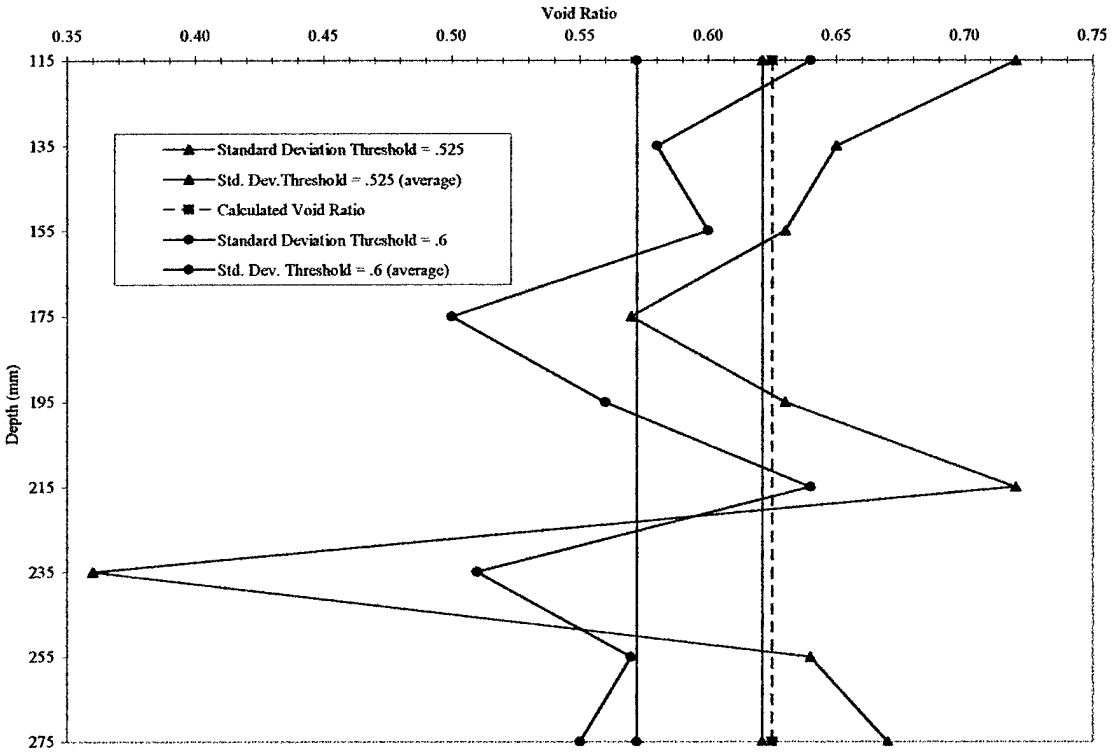

Chart 5. Calibration Sample #3: Method X

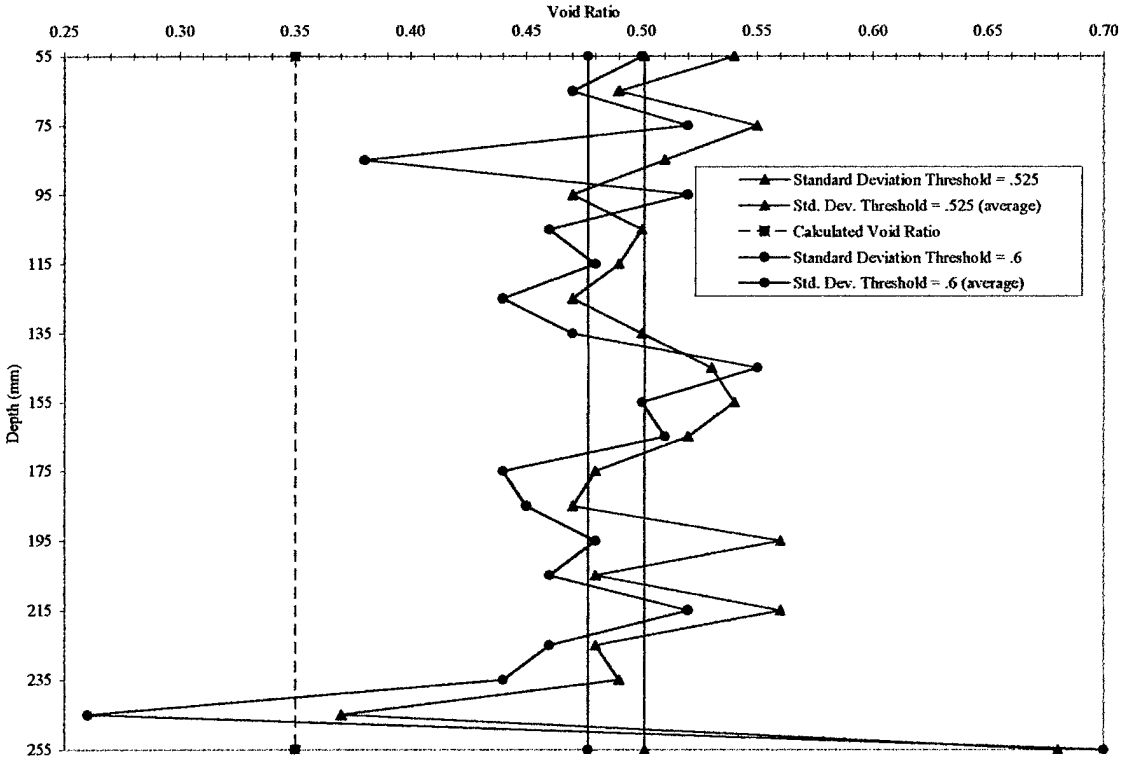

Chart 6. Calibration Sample #4: Method X

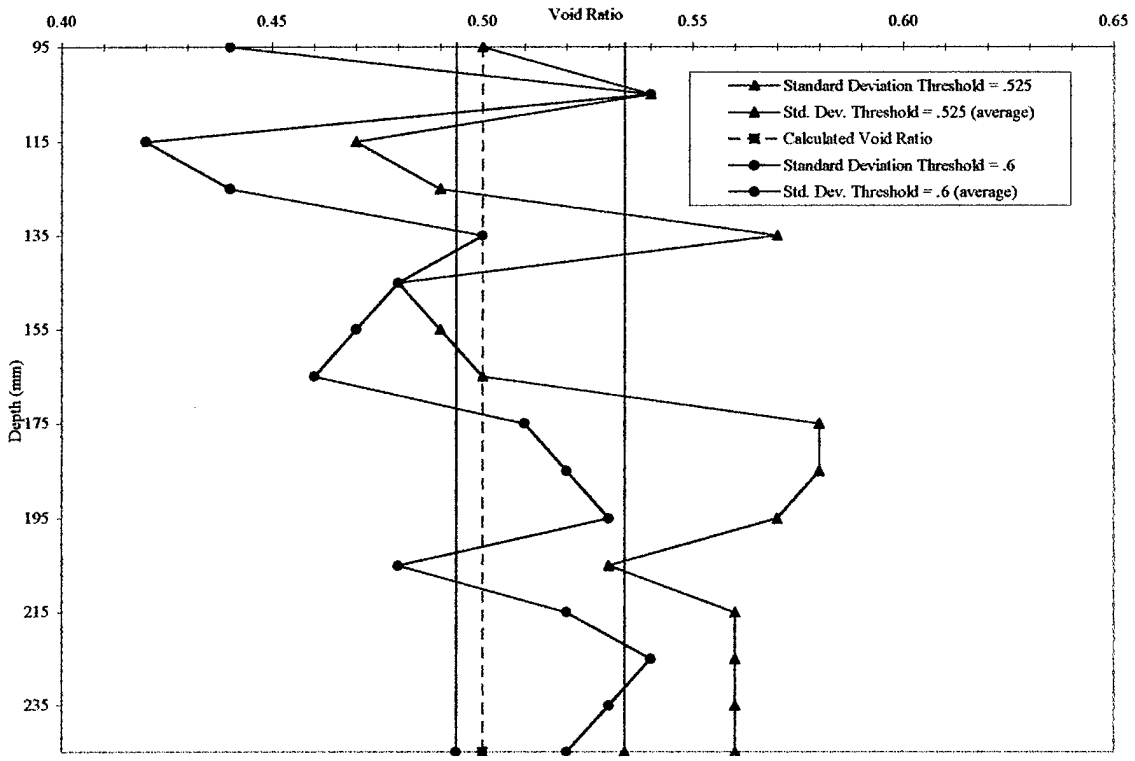

Chart 7. Calibration Sample #5: Method X

These charts show that a standard deviation threshold of .6 is a better fit across all three calibration cylinders than .525. Two of the average void ratios were overestimated and a third was pretty much even with the calculated void ratio with a standard deviation threshold value of .525. When the .6 value was used, one of the average void ratios was over, another a bit under, and the third pretty even with the calculated averages.

These charts also show that by no means is void ratio determination of soil samples via CAT an exact science. There are still many systematical bugs needing intense specialized study and research. While determination of the absolute void ratio is the ultimate desired outcome, this experiment required a consistent approach to see the distinctions between the reinforced and non-reinforced sections. Relative difference in void ratio was the basis for hypothesis testing.

Additional Scanning Considerations

One basic assumption in the image analysis methodology had broad effects. As discussed previously, the sample excavation method is the best available given the tools and implements available at Montana State. While working to a four-inch diameter sample was the obvious goal, a four-inch soil column could not be always obtained. In some instances the workable diameter was down as far as two inches. Though the frozen samples resulted in better specimens for analysis, the four-inch diameter could not always be obtained. The act of chiseling, by its very nature, leaves little room for uniformity of the specimen. The smaller cross-section images were then analyzed with the DR/CT scanner; unfortunately, a smaller area was available for interpretation.

The maximum amount of area was used in the void ratio determination for the soil cylinders from each test section. Regardless of the size of the area, the void ratio obtained from this area was taken to be the representative void ratio of the entire cross-section. Though the idea of weighting the void ratios obtained from larger cross-sections was hypothesized, it was eventually decided that the technique might influence the data when it was the sample retrieval method was to blame.

The calibrated void ratios took into account the entire soil cross-section present in a test cylinder. An additional investigation determined the void ratio based upon the inner two thirds of the sample only. The idea was that a lower void ratio should indeed be found in the interior without the cylinder wall to interfere with the packing.

As the chart below shows, the void ratio using a partial interior section was smaller than the void ratio of the whole cross-section. Because of the influence of the cylinder walls, more void spaces existed at the outer portions of the calibration samples.

The greater amount of void space at the interface of the cylinder wall is exhibited in the graph below.

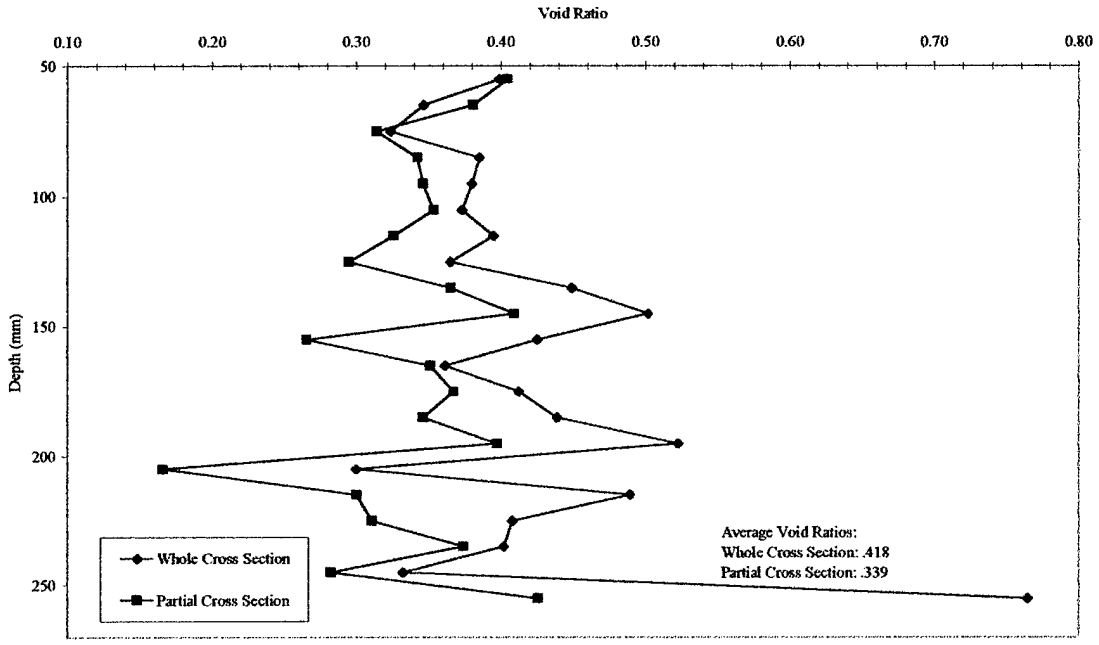

Chart 8. Calibration Sample #4: Whole Cross-Section versus Partial Cross-Section

CHAPTER 3: RESULTS

This chapter summarizes the results of the test sections based on density measurements, DCP testing, and CAT void ratio analysis.

Density Results

Table 3 lists the percent change in dry density for each reinforced and non-reinforced section. In addition, lift 1 and lift 2 values are separated for sections 3 and 4.

	Grid	No-Grid
Test Section #1	35.1	28.5
Test Section #2	43.5	55.0
Test Section #3		
Lift 1	40.1	26.2
Lift 2	34.0	30.6
Test Section #4		
Lift 1	28.7	37.6
Lift 2	45.1	32.6

Table 3. Average Percent Change in Dry Density for All Test Sections

Dynamic Cone Penetration Results

The DCP was used to evaluate the base course material in the effort to characterize as many physical characteristics as possible. The DCP measurements were converted to California Bearing Ratio (CBR) values, a characteristic routinely used to represent the support strength of subgrade material. The actual correlation between DCP value and CBR is shown in the following equation:

$$CBR = 292/(\text{DCP reading in millimeters per blow})^{1.12}$$

The following charts show base course CBR value versus depth for the test sections. Three DCP readings were taken in each half of the test box at locations A through F, the same locations as the nuclear densometer readings.

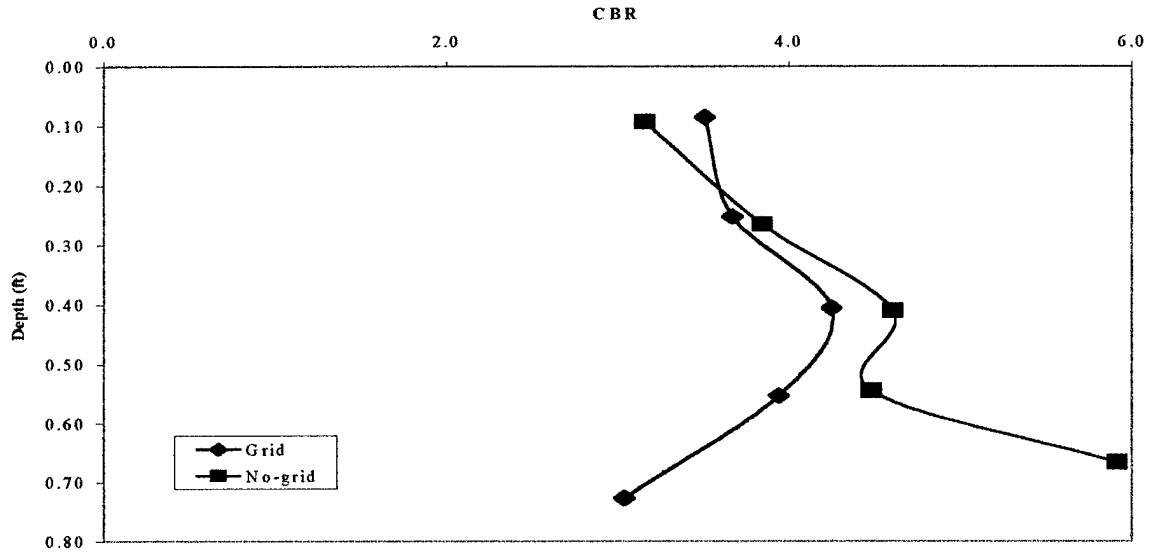

Chart 9. Test Section #1, Reinforced Base Course CBR (Average) vs. Non-Reinforced CBR (Average)

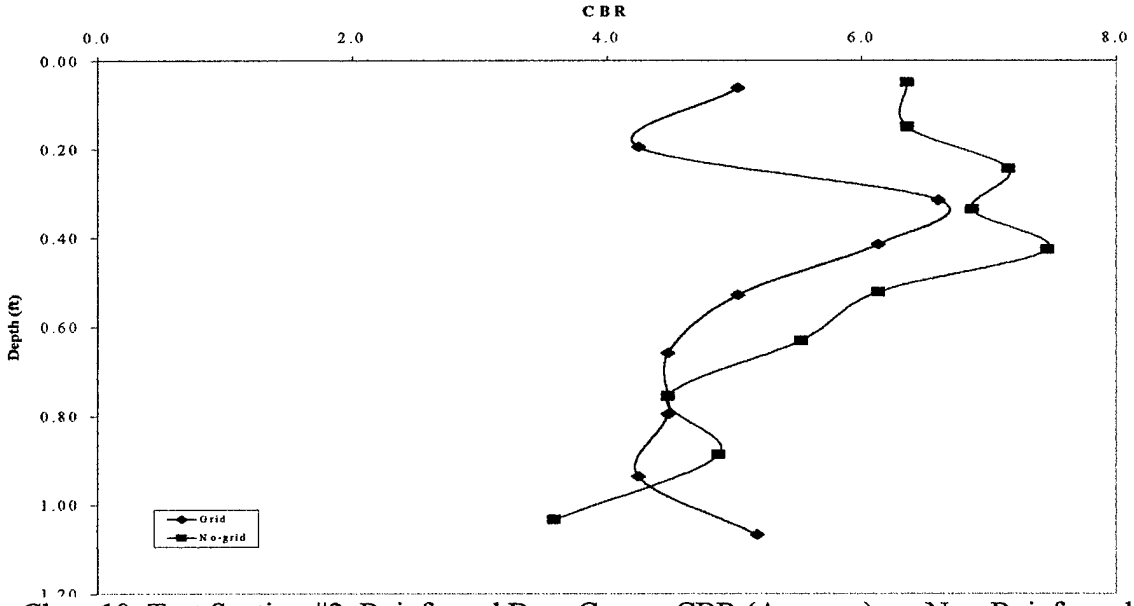

Chart 10. Test Section #2, Reinforced Base Course CBR (Average) vs. Non-Reinforced CBR (Average)

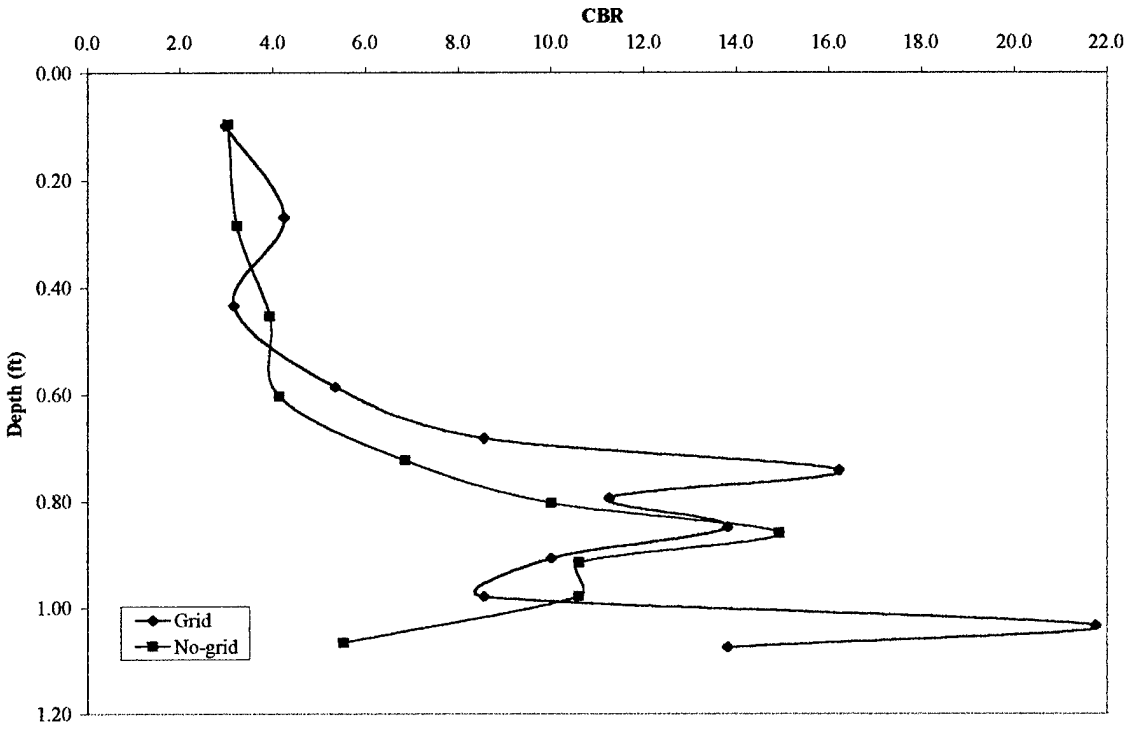

Chart 11. Test Section #3, Reinforced Base Course CBR (Average) vs. Non-Reinforced CBR (Average)

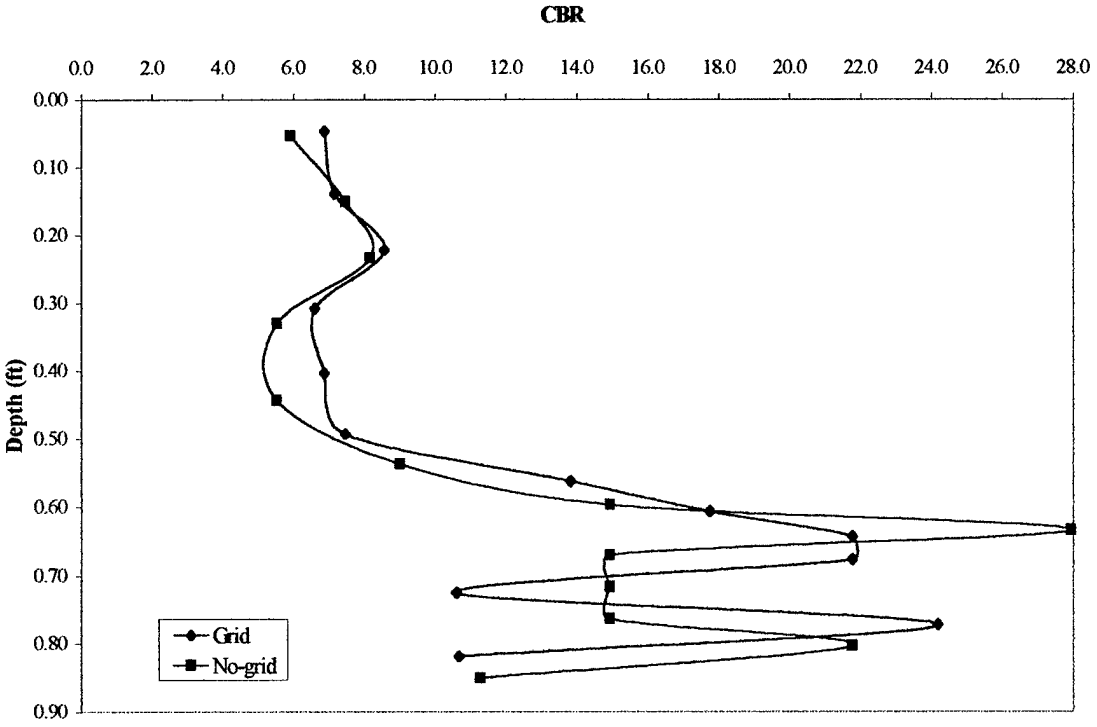

Chart 12. Test Section #4, Reinforced Base Course CBR (Average) vs. Non-Reinforced CBR (Average)

Computer-Aided Tomography Analysis

The CAT scanning analysis was performed on sections 3 and 4. Table 4 lists the results of the void ratio analysis for each core sample location to include the average void ratio, the standard deviation of the measurements, and the total number of scans for that particular soil column used in the analysis. Also included on the table are the combined averages that integrate core A with B and C with D.

		Ave. Void Ratio	Std. Dev.	# of Scans
Section #3	A	0.372	0.1284	27
	B	0.333	0.1522	26
	C	0.364	0.1115	28
	D	0.556	0.1716	29
Section #4	A	0.325	0.1462	23
	B	0.430	0.2676	28
	C	0.473	0.1695	28
	D	0.458	0.1944	27
COMBINED				
Section #3	Grid	0.353	0.1406	53
	No-Grid	0.462	0.1735	57
Section #4	Grid	0.383	0.2254	51
	No-Grid	0.466	0.1806	55

Table 4. Void Ratio Analysis Results for Test Sections 3 and 4

The following charts show the CAT analysis void ratios versus depth for each core sample location in sections 3 and 4. In addition to the void ratios at each point, the interface between the two lifts, the bottom of the base course material, and the average void ratio for the specific soil columns are also shown.

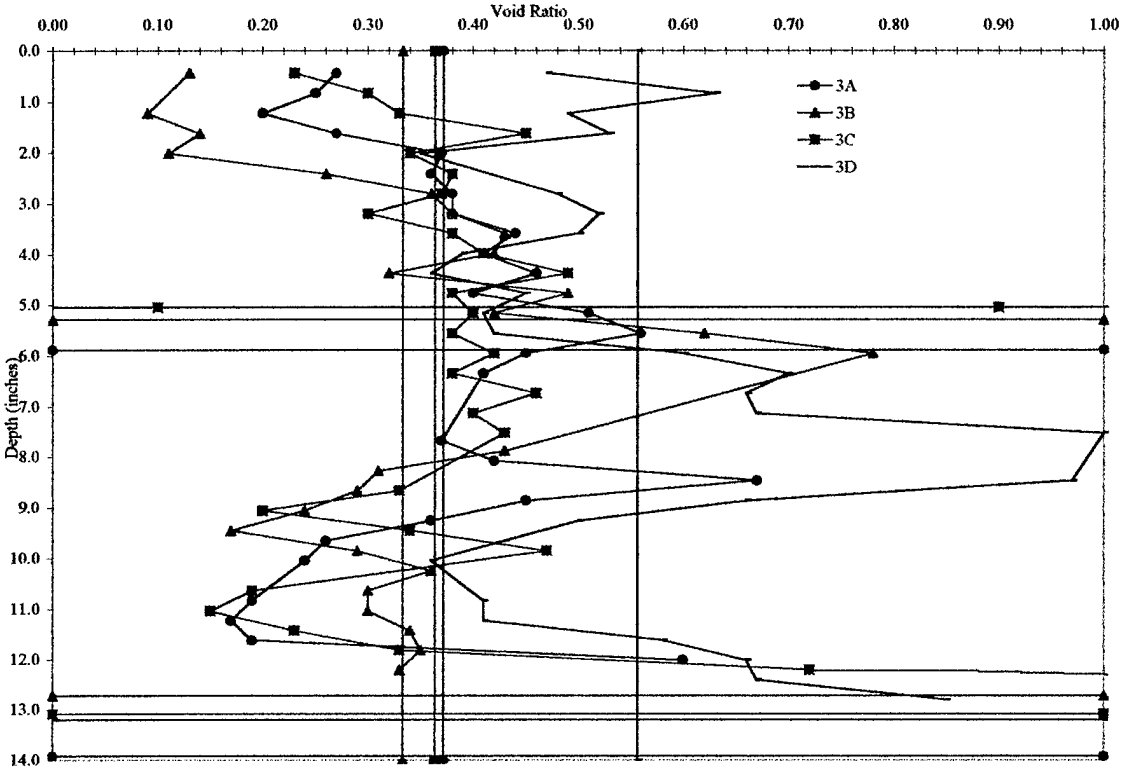

Chart 13. Test Section #3: Void Ratio vs. Depth for Sample Location A-D.

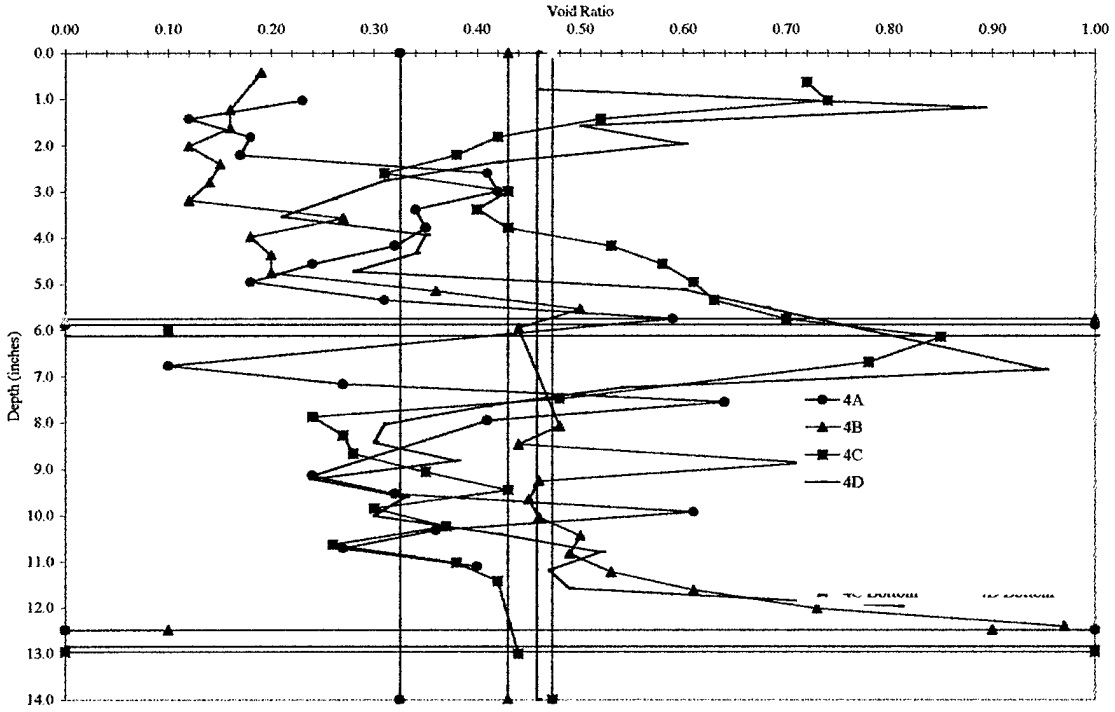

Chart 14. Test Section #4: Void Ratio vs. Depth for Sample Location A-D.

CHAPTER 4: INTERPRETATION OF RESULTS

Based upon review of density results and DCP measurements, there does not seem to be a clear indication that geogrid reinforced base course material achieves a greater density than non-reinforced material given the same amount of compactive effort. Four of the six lifts exhibited a greater change in density in the reinforced sections. Though a majority of the time the geogrid reinforced sections had a greater change in dry density, the results do not show that the geogrid significantly affects the compactive ability of the base course.

The DCP charts also show little distinction between the reinforced and non-reinforced base course, showing a consistent trend between CBR value and depth for both testable configurations. The non-reinforced base course typically has a greater CBR than the reinforced for most of the charts. Once again, there is no clear-cut difference to prove that the geogrid reinforced base course has achieved a higher density that the non-reinforced base course.

The void ratios obtained via CAT scan analysis do show a better distinction between the two configurations. The combined results as previously shown in Table 3 show a clear distinction between the average void ratio of the reinforced and non-reinforced base course. However, the variability seen in the various charts during the void ratio calibration and analysis procedures have highlighted the fact that the CAT scanning of soil samples leaves room for improvement.

Statistical techniques help to clarify any confusion about whether or not the void ratios for reinforced and non-reinforced sections are statistically different. This method, the "independent two-sample t-test", is based upon the means and standard deviations of

two independent samples. The distribution is a t-distribution; however, as the sample size approaches infinity, this distribution follows the more common "normal distribution".

The following equation is used in obtaining the t-statistic. This is the value that is then determines your confidence level in a t-distribution table.

$$t^* = \frac{\text{Grid void ratio mean} - \text{No-Grid void ratio mean}}{\sqrt{\left(\frac{\text{Grid variance}^2}{\text{Grid sample size}} + \frac{\text{No-Grid variance}^2}{\text{No-Grid sample size}}\right)}}$$

After calculating the above values and using the appropriate distribution table, I can conclude with 99.9% confidence for section three and 96% confidence for section four that the average void ratio for the reinforced sections is statistically different from the non-reinforced sections. These confidence levels show that the mean values for each of the testing configurations are significantly different from each other to allow for assignment of the above levels. The statistical inferences are based upon numerical characteristics only; they are blind to the experimental variation introduced by the testing administrator. This does not mean that for all CAT scanned samples the geogrid reinforced base course is guaranteed to have a lower void ratio. The confidence levels just state that for this particular sample's means and standard deviations, we can have this amount of confidence that the same analysis applied to the entire population will reveal the same result.

The testing of the central hypothesis in this experiment has shown that there is no significant increase in the compactive ability of a soil when a geogrid is included in the design for nuclear densometer and DCP results. However, the void ratio analysis results

do show a much better distinction. Statistical analysis reveals that geogrid reinforced base course can achieve a higher density than non-reinforced base course at a confidence level of at least 96%. Remember, this level is based upon the parameters found from this test only. Future testing could increase or lower this confidence level depending on the difference in means between the two configurations and their associated standard deviations.

CHAPTER 5: CONTRIBUTION TO CIVIL AND MILITARY ENGINEERING

The main contribution of this project is primarily the application of the various CAT scanning methods used to evaluate soil samples. Previous to this project no recorded CAT analysis had ever been performed to determine the density or void ratio of soil samples. This project has yielded tremendous information and lessons that could be used by future Montana State University students seeking to refine the CAT analysis process for soil samples. The analysis technique could be improved even more with the use and correlation of multiple calibration samples.

The geotechnical engineering profession may begin to use computer-aided tomography in future investigations. While CAT has been used previously in structural engineering and engineering mechanics, this research has shown that geotechnical engineering also has a utility for this technology. Perhaps other research projects will find ways to use CAT. The more this technology is studied and refined in research, the sooner it can reach the practice of geotechnical engineering.

Military engineering can benefit from the CAT methodology as well, but more direct application may be used in the design of future experiments evaluating the various benefits of geogrid in airfield and roadway design. The hypothesis that geogrid-reinforced base course can achieve a specific density faster than non-reinforced base course has tremendous implications for rapid military deployments that remain to be seen in the decades to come. The Armed Forces should look to similar studies as this in years to come to keep their deployment mobility at a maximum.

This research could be expanded in the future to more completely analyze this project's hypothesis. Should that occur, a few recommendations may prove to eliminate

most of the questions left by this experiment. The first would be to conduct even more calibration tests to make the void ratio analysis procedure even more precise. The method used so far is not the absolute best routine used; there is room for improvement.

The second recommendation is the scale of the test facility. A full-scale setup utilizing the same equipment, materials, and procedures as in normal highway construction should yield more consistent and realistic results. More samples could be taken for each configuration and would obviously increase the accuracy and reliability of the experiment.

Sidewalls affect the lateral movement of the base course. The hypothesis for this experiment was based on the fact that geogrid may decrease the amount of lateral movement in the base course; the sidewalls on the test box may have limited lateral movement somewhat and affected the true effects on the reinforced and non-reinforced sections. The construction of a test site without sidewalls, similar to that of a typical roadway, may better model the effect geogrid has on compaction.

This research project has opened a door for more intense study in the future. A larger quantity of test configurations will result in either backing up the conclusions of this particular project, refuting the results, or swing the door open even wider for more intensified testing. Either way, computer-aided tomography has made its entry into the geotechnical engineering research arena at Montana State University

Computer-aided tomography has shown to have great potential in civil and military engineering applications. This project represents an initial step to gradually bring CAT into a familiar format and methodology for future research and applications in the engineering world.

References

"Engineering Use of Geotextiles", Joint Departments of the Army and Air Force, TM 5-818-8/AFJMAN 32-1030, 20 July 1995.

Fannin, R. J. and Sigurdson, O. (1996) "Field Observations on Stabilization of Unpaved Roads With Geosynthetics", Journal of Geotechnical Engineering, Vol. 122, pp. 544-553.

Holtz, R. D. (1988) "Geosynthetics for Soil Improvement", Proceedings of the Symposium Sponsored by the Geotechnical Engineering Division of the American Society of Civil Engineers 1988, Special Publication No. 18, 211p.

John, N. W. M. (1997) "Geotextiles", Chapman and Hall: New York, 347p.

Kawamura, Toshiyuki. (1990) "Nondestructive, Three-Dimensional Density Measurements of Ice Core Samples by X-Ray Computed Tomography", Journal of Geophysical Research, August 10, 1990, Vol. 95, No. B8, pp. 12,407-12,412.

Koerner, R. M., and Soong, T. (1997) "The Evolution of Geosynthetics", Civil Engineering, Vol. 67, pp. 62-64.

Lynch, L. N., Webster, S. L., Bush III, A. J. (1996) "Expedient Surfaces", The Military Engineer, Aug/Sep 1996, pp. 32-33.

Moghaddas-Nejad, F. and Small, John C. (1996) "Effect of Geogrid Reinforcement in Model Track Tests on Pavements", Journal of Transportation Engineering, Vol. 122, pp. 468-74.

Perkins, S. W. (1999) "Geosynthetic Reinforced of Flexible Pavements: Laboratory Based Pavement Test Sections", Final Report for the State of Montana Department of Transportation, 17 March 1999.

Rao, P. V. (1998) "Statistical Research Methods in the Life Sciences", Duxbury Press: Boston.

Scudder, Henry J. "Introduction to Computer Aided Tomography", Proceedings of the IEEE, Vol. 66 No. 6, June 1978.

Van Santvoort, G. P. T. M. (1994) "Geotextiles and Geomembranes in Civil Engineering", A. A. Balkema: Rotterdam, Netherlands, 595p.

Van Santvoort, G. P. T. M. (1995) "Geosynthetics in Civil Engineering", A. A. Balkema: Rotterdam, Netherlands, 105p.

Appendix A

```
macro 'Soil Analysis';

var
  Count, Threshold:integer;
  StdDev,TheMean,MultFactor,nPixels,mean,mode,min,max:real;

begin
  copy;
  SetNewSize(700,700);
  MakeNewWindow('Binary');
  restoreroi;
  paste;
  EnhanceContrast;
  ApplyLUT;
  ResetGrayMap;
  MultFactor:= 0.6; {Change this number for calibration}
  ResetCounter;
  Measure;
  StdDev:=rStdDev[rCount];
  TheMean:=rMean[rCount];
  Threshold:=TheMean+round(MultFactor*StdDev);
  SetThreshold(Threshold);
  Showmessage('Threshold level =',Threshold,'\\Using ', MultFactor:4:3, ' standard
        deviations','\from the mean');
  MakeBinary;
  RequiresVersion(1.44);
  SetUser1Label('VoidRatio');
  Measure;
  GetResults(nPixels,mean,mode,min,max);
  rUser1[rCount]:=histogram[255]/histogram[0];
  UpdateResults;
  if (histogram[0]+histogram[255])<>nPixels
          then PutMessage('This macro requires a binary image.');
end;

macro '1. Image Setup Routine';
var
  Count, Threshold:integer;
  StdDev,TheMean,MultFactor:real;
begin
  Filter('smooth');
  Filter('median');
  SetScaling('Bilinear');
```

```
 SetScaling('New Window');
 ScaleAndRotate(0.5, 0.5 ,0);
 SubtractBackground('2D Rolling Ball', 15);
 Filter('median');
 ResetGrayMap;
 MultFactor:= 0.6; {Change this number if a change in calibration is needed}
 ResetCounter;
 Measure;
 StdDev:=rStdDev[rCount];
 TheMean:=rMean[rCount];
 Threshold:=TheMean+round(MultFactor*StdDev);
 SetThreshold(Threshold);
 Showmessage('Threshold level =',Threshold,'\\Using ', MultFactor:4:3, ' standard
       deviations','\from the mean');
end;

macro '2. Select your area';

begin
 Showmessage('Select the oval tool, hold SHIFT, and select your area');
End;

macro '3. Calculate Percent Voids';

var
 nPixels,mean,mode,min,max:real;

begin
 ApplyLUT;
 RequiresVersion(1.44);
 SetUser1Label('VoidRatio');
 Measure;
 GetResults(nPixels,mean,mode,min,max);
 rUser1[rCount]:=histogram[255]/histogram[0];
 UpdateResults;
 ShowResults;
 if (histogram[0]+histogram[255])<>nPixels
       then PutMessage('This macro requires a binary image.');
end;
```